

Francisco da Costa Rolo

# Study of the relative extraction efficiency of photocathodes in gaseous atmosphere

Dissertation for Integrated Master in Engineering Physics degree, submitted to Department of Physics of the Faculty of Sciences and Technology of University of Coimbra.

July 2016



UNIVERSIDADE DE COIMBRA



Faculty of Sciences and Technology  
University of Coimbra



Francisco da Costa Rolo

## **Study of the relative extraction efficiency of photocathodes in gaseous atmosphere**

Supervisor:

Prof. Dr<sup>a</sup>. Filipa Isabel Gouveia de Melo Borges Belo Soares

Dissertation for Integrated Master in Engineering Physics degree, submitted to  
Department of Physics of the Faculty of Sciences and Technology of University of  
Coimbra

July 2016

Esta cópia da tese é fornecida na condição de que quem a consulta reconhece que os direitos de autor são pertença da Universidade de Coimbra e que nenhuma citação ou informação obtida a partir dela pode ser publicada sem a referência apropriada.

This copy of the thesis has been supplied on condition that anyone who consults it is understood to recognize that its copyright rests with University of Coimbra and that no quotation from this thesis and no information derived from it may be published without proper acknowledgement.

This work was supported by FEDER, through Programa Operacional Factores de Competitividade-COMPETE and by National funds through FCT- Fundação para a Ciência e Tecnologia in the frame of Project QREN RAD4LIFE with the designation CENTRO-07-ST24-FEDER-002007. Francisco Rolo was also supported by this project.



# Abstract

Photocathodes are widely used in radiation detection since they convert photons into electrons by photoelectric effect. One of their most important characteristic is their Quantum Efficiency that is defined as the ratio between the number of incident photons and the number of emitted electrons.

Noble gases exhibit several properties that allow them to be chosen as detection media for some kinds of radiation detectors that also make use of photocathodes. In this conditions the electrons emitted by the photocathode interact with the gas and this might change the number of photoelectrons emitted, making it more accurate to talk in Extraction Efficiency instead of Quantum Efficiency.

Hence it is important to study the characteristics of photocathodes when they are placed in a gaseous atmosphere to optimize the performance of detectors that use them. Namely the effect of the photon incidence angle in the Extraction Efficiency can be an important issue and there is few data in the literature about this aspect motivated us to do this work.

In this work, an experimental system was designed, assembled and tested, and an experimental procedure was developed in order to study the influence of the photon incidence angle (between  $0^\circ$  and  $50^\circ$ ) in the Extraction Efficiency of photocathodes.

We performed this study for a Caesium Iodide photocathodes in Xenon at different pressures (between  $\frac{1}{2}$  and 5 bar).

It was found that the Relative Extraction Efficiency increases with the increase of the photon incidence angle for all the pressures and applied reduced electric fields, showing a behavior that is independent of the pressure of the gas and of the applied reduced electric field. It was also found that the variation of the Relative Extraction Efficiency with the reduced electric field presented the same behavior for all the photon incidence angle.

# Resumo

Os fotocátodos são amplamente utilizados em detecção de radiação, uma vez que convertem fótons em elétrons através de efeito fotoelétrico. Uma das suas características mais importantes é a sua Eficiência Quântica que é definida como a razão entre o número de fótons que nele incidem e o número de elétrons emitidos.

Os gases nobres apresentam várias propriedades que lhes permitem ser escolhidos como meio de detecção para alguns tipos de detetores de radiação que também utilizam fotocátodos. Nestas condições os elétrons emitidos pelo fotocátodo interagem com o gás e isso pode alterar o número de fotoelétrons emitidos, fazendo com que seja mais coerente referirmo-nos a Eficiência de Extração do que a Eficiência Quântica.

Assim, é importante estudar as características dos fotocátodos quando estes se encontram na presença de uma atmosfera gasosa para otimizar a performance dos detetores que os utilizam. Nomeadamente a dependência da Eficiência de Extração relativamente ao ângulo de incidência dos fótons pode ser uma questão importante além de que existe pouca informação disponível na literatura, o que motivou a realização deste trabalho.

Neste trabalho, um sistema experimental foi desenhado, montado e testado, e um procedimento experimental foi desenvolvido com vista a estudar a influência do ângulo de incidência (entre  $0^\circ$  e  $50^\circ$ ) na Eficiência de Extração de fotocátodos.

Foram estudados fotocátodos de Iodeto de Césio em Xénon a diferentes pressões (entre  $\frac{1}{2}$  e 5 bar).

Concluiu-se que a Eficiência de Extração Relativa aumenta com o aumento do ângulo de incidência dos fótons para todas as pressões e campos elétrico reduzidos aplicados, mostrando um comportamento que é independente da pressão do gás e do campo elétrico reduzido aplicado. Também se concluiu que a variação da Eficiência de Extração Relativa com o campo elétrico reduzido apresenta o mesmo comportamento para todos os ângulos de incidência dos fótons.

# Acknowledgements

This work was made possible through the help of many people to whom I would like to thank.

I would like to especially thank my supervisor Prof. Dr<sup>a</sup>. Filipa Borges, for all the guidance, patience and help she provided me. Without it this work would not be possible.

Also to Dr. Kiwamu Saito, for all the help in the early stages of this work.

To Alexandre Trindade for all the help in the laboratory, and to André Cortez and Dr. Conde for all the hints and tips.

I would like to sincerely thank to all my colleagues, especially to André, Bruno, Daniel, Mariana, Olivier and Pedro for all the life, fun and learning that we did together.

To my family that supported and influenced me the most.

And last, but not least, to my Marianinha Fofinha, for everything, but especially for showing me that life is better with love.

Thank you all.

# Publications

## Oral communications

1. F. C. Rolo, et al., “High pressure Xenon doped mixtures for the Next collaboration – Study of Quantum Efficiency dependence of photocathodes with light incidence angle at high pressure”, oral presentation, Jornadas Científicas do LIP, 19<sup>th</sup> to 21<sup>st</sup> February 2016, Universidade do Minho, Braga, Portugal
2. F. C. Rolo, et al., “Dependence on the incident angle and pressure of the Relative Extraction Efficiency of photoelectrons from a CsI photocathode”, oral presentation, RD51 Collaboration Meeting, 8<sup>th</sup> to 11<sup>th</sup> March 2016, CERN, Switzerland

## Poster communications

1. K. Saito, et al., “Study of the dependence of the Quantum Efficiency of a CsI photocathode”, poster presentation, International Symposium on Radiation Detectors and Their Uses, 18<sup>th</sup> to 21<sup>st</sup> January 2016, KEK, Tsukuba, Japan
2. F. C. Rolo, et al., “Variation of the effective Quantum Efficiency of CsI photocathodes with the incidence angle”, Apresentação Intercalar dos projectos de MIEF, 17<sup>th</sup> of February 2016, Universidade de Coimbra, Portugal

## Future poster communications

3. F. C. Rolo, et al., “Quantum Efficiency Dependence of a CsI Photocathode with Photon Incidence Angle”, 2016 IEEE Nuclear Science Symposium, 29<sup>th</sup> of October to 6<sup>th</sup> November 2016, Strasbourg, France



# Contents

<b>1. INTRODUCTION .....</b>	<b>1</b>
<b>2. BACKGROUND CONCEPT.....</b>	<b>3</b>
2.1 NOBLE GASES AS DETECTION MEDIA .....	3
2.2 PHOTOCATHODES AND THEIR APPLICATIONS .....	4
2.3 PHOTOELECTRON EMISSION .....	4
2.4 PHOTOCATHODE TYPES.....	9
2.5 PHOTOCATHODES IN GASEOUS ATMOSPHERES .....	11
2.6 CSI PHOTOCATHODES.....	13
2.7 QUANTUM EFFICIENCY VARIATION WITH THE INCIDENCE ANGLE .....	14
<b>3. EXPERIMENTAL SYSTEM .....</b>	<b>16</b>
3.1 OPERATION PRINCIPLE.....	16
3.2 EXPERIMENTAL SETUP.....	17
3.3 VACUUM AND GAS INSERTION LINE .....	21
3.4 CSI PHOTOCATHODE.....	24
<b>4. METHODOLOGY .....</b>	<b>25</b>
4.1 GENERAL DESCRIPTION .....	25
4.2 DARK CURRENT .....	28
4.3 UNCERTAINTY AND ERROR PROPAGATION.....	28
<b>5. EXPERIMENTAL RESULTS AND DISCUSSION .....</b>	<b>30</b>
5.1 REE VARIATION WITH THE INCIDENCE ANGLE FOR CONSTANT E/P .....	30
5.2 REE VARIATION WITH E/P FOR A CONSTANT PHOTON INCIDENCE ANGLE.....	34
5.3 REPRODUCIBILITY.....	40
<b>6. CONCLUSION .....</b>	<b>41</b>
<b>7. FUTURE WORK.....</b>	<b>43</b>
<b>8. REFERENCES.....</b>	<b>45</b>

## Figures Index

Figure 2. 1 - Energy diagram for the emission of photoelectrons in metals.....	6
Figure 2. 2 - Band diagram for the emission of electrons in semiconductors .....	7
Figure 2. 3 - Band diagram for the diverse types of semiconductors: (n) - n-doped; (i) - intrinsic; (p) - p-doped .....	8
Figure 2. 4 - Schematic representation of the operation modes of a photocathode. a) Reflective; b) transmissive .....	10
Figure 2. 5 - Example of two photocurrent measurements obtained in vacuum (o) and with 2 bar of argon (□) .....	12

Figure 2. 6 - Photoelectron-collection efficiency of a CsI photocathode in Ar and CH4 as a function of the reduced applied field .....	12
Figure 2. 7 - Quantum Efficiency of CsI as function of wavelength of incident photons .....	13
Figure 2. 8 - Results obtained by a) Lopes and Conde (1993); b) Miné et al. (1995); c) Tremsin and Siegmund (1999) .....	15
Figure 3. 1 - Schematic of the operational principle of the experimental system.	16
Figure 3. 2 - a) Spectral distribution of the Deuterium Lamp; b) Spectral Responce of CsI photocathodes .....	17
Figure 3. 3 - Schematic of the experimental system designed in Solidworks .....	18
Figure 3. 4 - Simulation performed by Solidworks of the deformation that the main chamber of the experimental system at 20 bar.....	19
Figure 3. 5 - Angle variation device. a) Schematic designed in Solidworks; b) Photograph during the assembly of the experimental system.....	20
Figure 3. 6 - Schematic of the set up that allows the production and collection of the electrons.....	20
Figure 3. 7 - Schematic of the gas and vacuum line.....	23
Figure 3. 8 - Photograph of the experimental sytem.....	23
Figure 4. 1 - Behaviour of the signal produced by the photocathode over time. At orange, with the upper chamber being evacuated. At blue, with the upper chamber closed, after being evacuated.....	26
Figure 4. 2 - Schematic of how a measurement was performed .....	27
Figure 5. 1 - Obtained results for REE variation with the incidence angle for different E/p values at 0,5 bar of Xe. Values are relative to the 0° incidence angle .....	31
Figure 5. 2 - Obtained results for REE variation with the incidence angle for different E/p values at 1 bar of Xe. Values are relative to the 0° incidence angle .....	31
Figure 5. 3 - Obtained results for REE variation with the incidence angle for different E/p values at 2 bar of Xe. Values are relative to the 0° incidence angle. ....	32
Figure 5. 4 - Obtained results for REE variation with the incidence angle for different E/p values at 3 bar of Xe. Values are relative to the 0° incidence angle .....	32
Figure 5. 5 - Obtained results for REE variation with the incidence angle for different E/p values at 4 bar of Xe. Values are relative to the 0° incidence angle .....	33
Figure 5. 6 - Obtained results for REE variation with the incidence angle for different E/p values at 5 bar of Xe. Values are relative to the 0° incidence angle .....	33
Figure 5. 7 - Obtained results for REE variation with E/p for a constant photon incidence angle at 0,5 bar of Xe. Here, the two measurements are coincident .....	35

Figure 5. 8 - Obtained results for REE variation with E/p for a constant photon incidence angle at 1 bar of Xe.....	35
Figure 5. 9 - Obtained results for REE variation with E/p for a constant photon incidence angle at 2 bar of Xe.....	36
Figure 5. 10 - Obtained results for REE variation with E/p for a constant photon incidence angle at 3 bar of Xe.....	36
Figure 5. 11 - Obtained results for REE variation with E/p for a constant photon incidence angle at 4 bar of Xe.....	37
Figure 5. 12 - Obtained results for REE variation with E/p for a constant photon incidence angle at 5 bar of Xe.....	37

# 1. Introduction

Radiation detection instrumentation is a field with extensive applications like medical imaging, material analysis, high energy physics, astrophysics and space applications.

In particular, gas radiation detectors are based on the interactions of the incoming radiation with noble gas atoms that might translate into the production of charge or electroluminescence (typically in the Vacuum Ultra-Violet region). One of the aspects that is considered in the detectors that use electroluminescence as an amplification stage is the efficiency of detection of this light by the light converter, namely the photocathode.

For some applications, namely for high energy applications (above about  $\sim 100$  keV), in order to maximize the performance of these gaseous detectors, the number of interactions can be maximized by increasing the density of targets which can be obtained by increasing the gas pressure.

Noble gas electroluminescence, which is used in gas proportional scintillation counters (GPSC), and Ring-imaging Cherenkov (RICH) detectors are examples of applications for which the study of devices based on VUV photocathodes is important.

Photocathodes are widely used in radiation detection since they convert photons in electrons by photoelectric effect. One of the most used photocathode material is Caesium Iodide (CsI), which has its spectral response in the VUV region and has one of the highest quantum efficiency among its competitors.

When operated in gaseous atmospheres there are some effects that should be addressed to collect the emitted photoelectrons. In fact, these might be backscattered to the photocathode or might excite the gas atoms which will lead to photon-feedback.

Hence, the study presented emerges from the importance of studying the properties of photocathodes when enclosed in a gaseous atmosphere, in order to improve the performance of detectors that use them. This subject has been studied for a long time by various authors and many aspects of it have already been covered. Nonetheless when considering high pressure gases (above about 5 atm), the dependence of the quantum efficiency with the photon incidence angle, and the influence of the substrate on which the photocathode film is deposited, few information is available in the literature [16-18]



and the existing results are not always consistent with each other. Also no study of the influence of the photon incidence angle was found for photocathodes in a gaseous atmosphere.

Therefore, the aim of this work was the study of the variation of the Extraction Efficiency with the photon incidence angle of photocathodes in gaseous atmosphere at a range of pressures from 0,5 to 5 bar and for different substrate material.

For this purpose, an experimental system that allows the study of the dependence of the characteristics of reflective photocathodes with the variation of the photon incidence angle, gas pressure and substrate was designed and assembled.

The system is able to sustain high pressures and is flexible enough to allow the study of the above referred characteristics of photocathodes, namely by varying the photon incidence angle.

In **chapter 2**, the most significant concepts are explained and some of the published results that are important for this study are presented. In **chapter 3**, the experimental setup that was designed is described and explained, while in **chapter 4**, the experimental procedure and the reasons for the options chosen are discussed. In **chapter 5**, the results obtained are presented and the discussion of these is made, while **chapter 6** is dedicated to the conclusions. At last, in **chapter 7**, some suggestions are made for future work that might arise from my own.

## 2. Background Concepts

### 2.1 Noble Gases as Detection media

The most important characteristic of a detection media is its ability to stop and absorb radiation and transform it into charge or photon emission.

Noble gases have several advantages that make them very attractive as detection media. They exhibit small Fano factor (that quantifies the statistical fluctuations in the processes of energy to charge conversion) and, for those with high atomic number, high stopping power and low ionization energy. Also, being gases, they are reasonably easy to handle and easy to adapt to the geometry of detectors.

When incident particles interact with the gas, the kind of interactions that take place depend on the type of incident particles. Charged particles like electrons or alpha particles might ionize the atoms of the gas, originating an electron-ion pair, and if the electrons removed have sufficient energy they can ionize other atoms and these might do the same and so on. This behaviour might be enhanced if an electric field is applied that accelerates the electrons to compensate the energy lost by them in the ionization process and to ensure they have enough energy to originate new ionizations. This behaviour is the basic idea behind proportional counters. [1,2]

If electrons don't have enough energy for ionization to occur, they might just excite the atoms of the gas. The excitation process raises an electron to a higher energy state and when it returns to its original state this process results in the emission of photons with characteristic energies. The excitation energy released in this process is typically in the VUV region.

If the incident particles are photons, these interact by photoelectric effect, Compton scattering or pair production. The probability of these processes to occur depends on the energy of the incident radiation and on the atomic number of the target.

Xenon, with its high atomic number ( $Z = 54$ ), is an excellent candidate as a noble gas detection media, since it has a higher cross section and a lower ionization potential due to its high atomic number. [1,2]

## **2.2 Photocathodes and their applications**

A photocathode is a material that converts light into electrical charge. This is, when photons strike a photocathode, it responds by emitting electrons, through photoelectric effect.

The most important characteristic of a photocathode is the one that relates the quantity of light that irradiates the photocathode and the quantity of electrons that it emits. This characteristic is called Quantum Efficiency (Q. E.) and is defined as the following ratio:

$$Q.E. = \frac{\# \text{ emitted electrons}}{\# \text{ incident photons}}$$

Despite the Q.E., there are other important properties that characterize photocathodes, such as the resistance to radiation exposure without their degradation (aging), tolerance to the exposure to strange elements, and response time.

During many years, photocathodes were the only practical method of light conversion into electric charge. Hence, its applications are very wide, ranging from academic purposes to everyday. Photocathodes are the main component for optoelectronic devices, such as TV camera tubes and image tubes. Radiation detectors based in photocathodes are used in diverse applications. Examples in particle physics are RICH detectors, scintillation detectors, calorimeters or particle tracking systems; in medical imagology they are used in Gamma chambers, SPECT and PET. More recently, the development of solid state devices, such as the photodiode, compete with the use of photocathodes in some applications. [2]

## **2.3 Photoelectron Emission**

An incident photon interacting with a photosensitive material results in the conversion of the photon into an electron emitted by photoelectric effect.

The number of emitted electrons only depends on the intensity of the incident light, while their energy depends only on the frequency of the light (the higher the frequency, the higher the energy of the photons). The theory of photoelectric effect was formulated by Einstein in 1905 [4] and according to it, the highest energy of the emitted electron in this process might be calculated through:

$$E_K = h\nu - E_{min}$$

where  $E_K$  is the kinetic energy of the emitted electron,  $h\nu$  is the energy of the incident light and  $E_{min}$  is the minimum energy to remove an electron from the surface of the material.

In 1958 Edward Spicer came up with a theory that explains the differences of the quantum efficiency of different materials. [5] According to this theory the process of emitting an electron occurs in three steps:

1. Absorption of the incident photon by a photosensitive material, with the ionization of an atom of the material;
2. Diffusion of the electron inside material to its surface;
3. Escape of the electron through the potential barrier on the surface (related with the electron affinity) to the vacuum.<sup>1</sup>

This models gives a description of the process of electron emission, relating the process with the characteristics of the material, like the optical absorption, electron scattering inside the material and the electron affinity.

Each step of the process originates energy losses. In the first step there may be some photons that are not absorbed by the material. These photons may be lost because of the light reflection in the material. In the second step energy is lost due to electron scattering through collisions with other electrons or with phonons. In the third step, some of the electrons that reach the surface, are not energetic enough to overcome the potential barrier of the surface. Hence the materials that have better quantum efficiency, that is, that have higher electron emission per incident photon, are the ones that have less energy loss in these steps of the emission process.

Metals are known for their inefficiency in this process. Firstly, they are typically highly reflective, so the ionization of electrons is very low due to the fact that few photons contribute to it. Secondly, in their path to the surface, excited electrons lose a lot of energy in electron-electron collisions. Therefore, only electrons that are excited near the surface have probability of escaping the metal, as can be seen in the **Figure 2.1**. Lastly, the electron affinity energy,  $E_A$ , that in solid state physics is defined as the energy obtained by moving an electron from the vacuum just outside the material to the bottom of the

---

<sup>1</sup> In Band Theory it is common to refer vacuum the exterior of the material, even when this is not in the void.



conduction band, for most metals is higher than 2 eV, which is a high value for electrons, when compared with their thermal energy (~25 meV) [3]

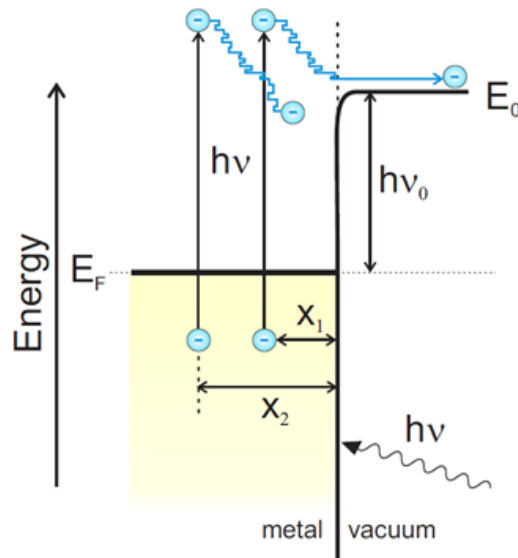


Figure 2. 1 - Energy diagram for the emission of photoelectrons in metals [3]

As we can see in the **Figure 2.1**, the minimum energy for extracting an electron might be given as:

$$E_{min} = \Phi = E_0 - E_F = h\nu_0$$

where  $E_F$  is the Fermi energy (energy of the occupied state with the higher energy associated) and  $E_0$  is the surface potential barrier (typically between 2 and 6 eV).

Contrary to metals, semiconductors are much more efficient in photoelectron emission. Their reflection coefficient is typically low, while the photon penetration length (for photon energies higher than the gap energy,  $E_G$ ) is high. Also, in semiconductors, electrons traveling to the surface of the material are scattered, mainly by collisions with phonons which leads to small energy losses in this process. In semiconductors, electrons that are excited in a distance to the surface of a few hundreds of Å, have enough energy to escape the material. In **Figure 2.2** the potential barrier considerations can be better understood using the band diagram.



of escape of the electrons,  $l_e$ , is higher than the thickness of the bending of the band,  $l_e \gg x_0$ , it means that electrons excited deep in the semiconductor are the ones that will be emitted, then, the level of vacuum for these electrons is higher due to the electric field produced by the surface dipole. This leading to  $E_{min}$  to be increased by an energy amount  $\Delta E$  for electrons that are excited deeper than  $x_0$ . Therefore, n-doped semiconductors result in photocathodes with a low Q.E. In **Figure 2.3 (n)** there is a schematic that can be used to make these words much more clear, concerning a n-doped semiconductor.

Concerning a p-doped semiconductor, we get an analogous situation, but with the “band bending” occurring downwards, that is, instead of  $E_{min}$  being increased by an energy amount  $\Delta E$ , it decreases by the same amount. This leads to an easier electron emission in a p-doped semiconductor when compared to the other semiconductor types. In **Figure 2.3 (p)** this situation is represented schematically.

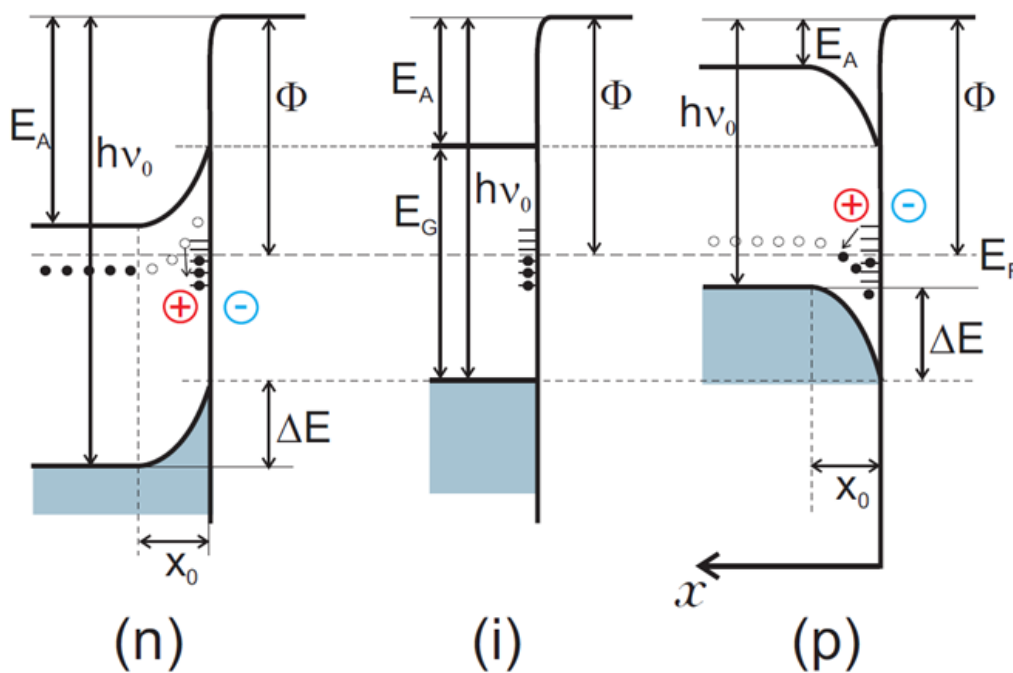


Figure 2.3 - Band diagram for the diverse types of semiconductors: (n) - n-doped; (i) - intrinsic; (p) - p-doped [3]

It became clear that the p-doped semiconductors are the best photoelectron emitters as they have a lower value of  $E_{min}$ .

Now suppose that we have a photon with energy slightly higher than  $E_{min}$ . So this photon has enough energy to excite an electron from the top of the valence band to the vacuum level. Arriving to the conduction band that is after losing a share of its energy

equal to  $E_G$ , it is designated by “hot electron” and it has an excess of energy  $E_A$  (relatively to the required to be on the conduction band). In this case there are two possible scenarios, regarding the ratio between the energy of the band gap,  $E_G$  and the electronic affinity,  $E_A$ :

If  $E_G/E_A > 1$ , the electron has an high probability of escaping, because the only other way to lose energy is having collisions with the atoms of the lattice, which is a very inefficient way to lose energy;

If, on the other hand,  $E_G/E_A < 1$ , the electron has energy enough to escape or to raise another electron from the valence band to the conduction band. In the second case, neither will have enough energy to escape after the promotion of the second electron. Experiments have shown that electron-hole production is a more probable process than electron emission.

Hence, semiconductors with  $E_G/E_A > 1$  tend to have an higher Q.E. than the ones with  $E_G/E_A < 1$ .

## **2.4 Photocathode Types**

Generally, a photocathode is a photosensitive semiconductor film, deposited in a substrate which can operate in a reflective (opaque) configuration or in a transmissive (semi-transparent) configuration. In the case of a reflective photocathode, the photons strike the photocathode in the same side where the electrons are emitted, while in a transmissive photocathode, the photons strike the substrate of photocathode, and, the electrons are emitted by the photocathode in the opposite side.



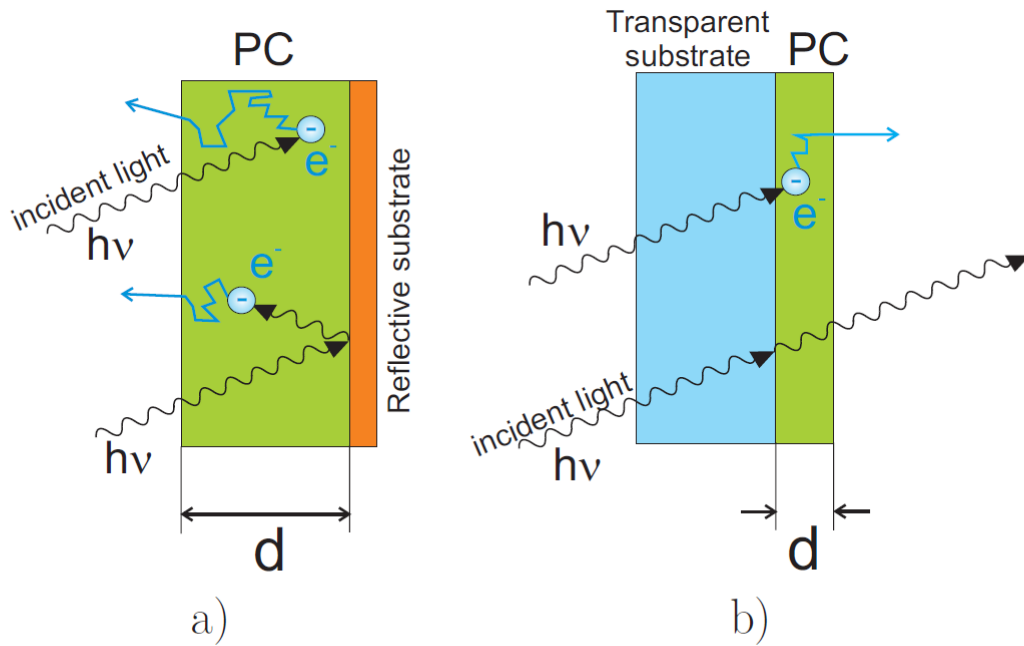


Figure 2. 4 - Schematic representation of the operation modes of a photocathode. a) Reflective; b) Transmissive [3]

For transmissive photocathodes, their thickness is a very critical characteristic. If the thickness is too large, the electrons might not have enough energy to escape the photocathode, but if it is too small then the photons might go through it without being absorbed. Hence, the optimal thickness of a transmissive photocathode is a value that depends on the absorption of the material and on the escape depth of the ionized electrons. Both this factors are dependent on the wavelength of the incident light, increasing as the wavelength decreases. Hence, the ideal value of thickness represents a compromise between the loss of photons through transmission without ionization of electrons, and the number of electrons that are excited too far away of the surface that and cannot escape from it. As a result, the spectral response of a transmissive photocathode might be modified to a certain extent, through manipulation of the optimal thickness for each spectral region.

For reflective photocathodes, the thickness is not so critical. If the photocathode is deposited onto a reflective substrate, the incident light that is not absorbed by the photocathode is reflected in the substrate and has another chance to excite an electron. This leads to an increased value of the Q.E. since the absorption of light can be optimised without having a big impact on the escape length of electrons. Thus reflective photocathodes tend to be easier to produce since the thickness requirement is not very demanding. [3,7]

## **2.5 Photocathodes in gaseous atmospheres**

When in presence of a gaseous atmosphere, there are a couple of important aspects that we will now refer to.

In vacuum environment, after leaving the photocathode surface, the emitted electrons have nothing to interact with. The same does not occur in presence of a gaseous atmosphere. The interactions between the emitted electrons and the gas atoms/molecules might be different depending on the energy of the electrons.

Hence, when these collide with the atoms/molecules of the gas, they may be backscattered and if this occurs in the region near the photocathode, the electrons might be reabsorbed by it, leading to a decrease in the number of photoelectrons available to be collected.

On the other hand, when the electrons have enough energy, they excite the atoms/molecules of the gas and in the process of de-excitation these emit photons (electroluminescence) that might cause photoelectron emission by the photocathode therefore, increasing the number of photoelectrons produced. This phenomenon is called photon-feedback, and there is an energy threshold, typical for each gas for it to occur.

One way to increase the number of collected photoelectrons is to apply an electric field,  $E$ , used to drive and increase the energy of the photoelectrons emitted by the photocathode (beyond the energy they already have when escaping). Also, the number of the collected photoelectron is dependent of the pressure of the gas,  $p$ . But, we can compensate this by scaling the applied electric field with the pressure. This leads to being more common to see these studies described as function of the Reduced Electric Field,  $E/p$ , whose unit of measurement is  $V \cdot cm^{-1} \cdot Torr^{-1}$ . But the pressure of the gas depends on its temperature, then, it is also common to withdraw the temperature dependence by dividing the electric field by the concentration of atoms/molecules of the gas. In this case the reduced electric field is  $E/N$  and is measured in Townsend,  $Td$  ( $1 Td = 10^{-21} V \cdot m^2$ ).

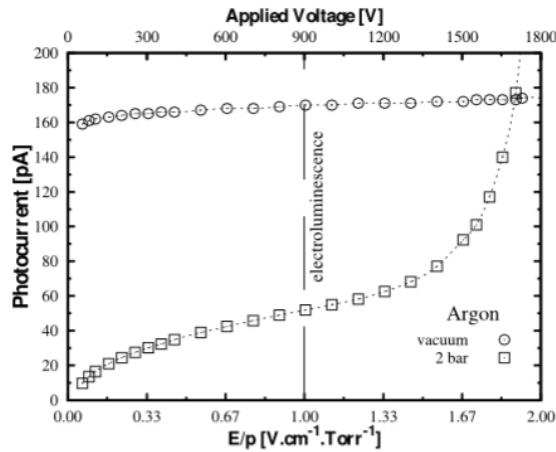


Figure 2. 5 - Example of two photocurrent measurements obtained in vacuum (o) and with 2 bar of argon (□) [8]

In noble gases, such as, Argon or Xenon, the inelastic threshold is high when compared to molecular gases, so collisions with their atoms are mainly elastic ones leading to an increase of backscattering. Thus with these gases a low extraction efficiency is expected. On the other hand, for molecular gases, the inelastic threshold is much lower due to vibrational and rotational transition channels [9, 10]. **Figure 2.6** shows the contrast between experimental results of the extraction efficiency of a noble gas (Ar) and an molecular one ( $CH_4$ ). Somewhere around  $E/p = 1,5 V \cdot cm^{-1} \cdot Torr^{-1}$  we can see, for argon, the change of behaviour, related with the threshold for photon-feedback.

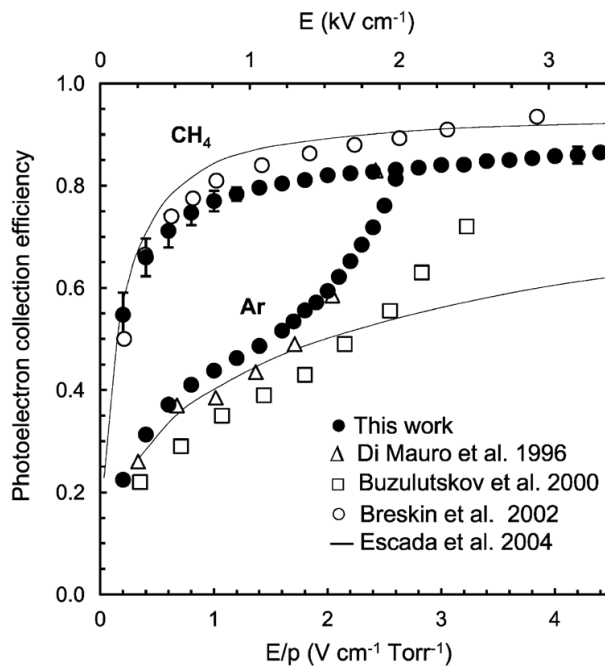


Figure 2. 6 - Photoelectron-collection efficiency of a CsI photocathode in Ar and  $CH_4$  as a function of the reduced applied field [11]

Since these issues originate a difference between the number of electrons that are emitted by the photocathode and the number of electron that are collected, it is more accurate to talk in Effective Extraction Efficiency (or Photoelectron Extraction Efficiency) instead of Quantum Efficiency. This quantity is known to depend on gas/mixture and reduced electric field [9,10].

## **2.6 CsI Photocathodes**

Caesium Iodide is a semiconductor which is known to be an efficient photocathode in VUV region of the electromagnetic spectrum.

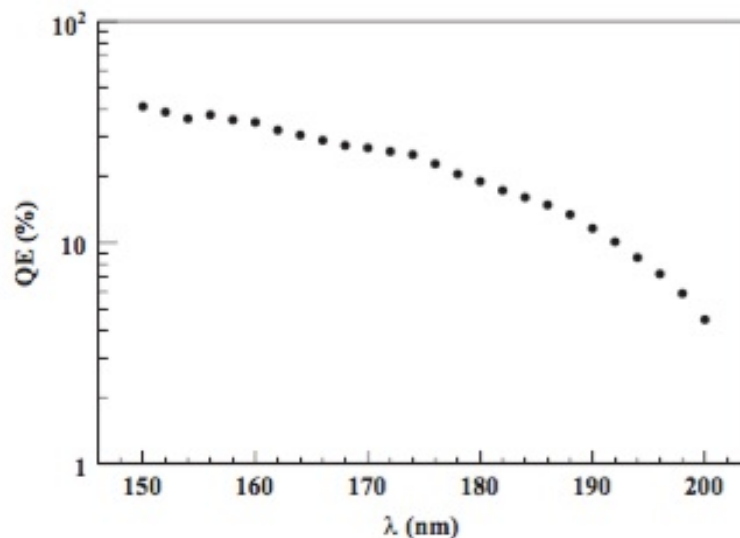


Figure 2. 7 - Quantum Efficiency of CsI as function of wavelength of incident photons [12]

Its spectral response is limited to 210 *nm* since its gap energy is approximately 6 *eV*[10]. Therefore, CsI is not sensible to the visible light, which allows an operation without big concerns with light isolation. In fact, Triloki et al. showed in 2015 [12] that CsI is almost transparent in the 225 – 900 *nm* region and opaque in the 190 – 225 *nm* region. It also has an electron affinity of around 0,1 to 0,2 *eV* [10], which explains its high quantum efficiency, since the condition  $E_G/E_A > 1$  mentioned in the section 2.3, is satisfied.

Also, CsI photocathodes exhibit other features which make their use quite convenient. They have a high resistivity, of the order  $10^{10} - 10^{11} \Omega \cdot cm$  [13] which allows them to be stable when operated at high radiation fluxes. Their radiation hardness [14] is important for long term operation in high radiation intensity environments and they are easy to produce by evaporation in vacuum, although some cautions must be taken, like increasing the evaporation rate for poor vacuum conditions, to minimize contamination [10], for example.

They are stable in gaseous atmospheres except in presence of water, since they are hygroscopic. This last feature allows them to be exposed to air just for a few minutes which is very useful in terms of the experimental assembly, since it allows the photocathode to be produced in a special purpose set up and then transported to the experimental system.

When working with CsI photocathodes, it is important to have knowledge of the principal causes of degradation of the Q.E. of the photocathode. This effect is usually called photocathode aging. For this study the more relevant ones are the exposure to humidity [10, 15] and intense photon flux [10]. In both cases increasing the temperature of the photocathode (heat-treating) can bring some reversibility to the process.

### **2.7 Quantum Efficiency variation with the incidence angle**

The incidence of light in a photocathode may not always be perpendicular to its surface, in the most common applications. Hence it is important to know what are the changes observed when the incidence angle of the photons varies.

In 1993 Lopes and Conde [16] observed an increase of 30% for the quantum efficiency for some chevron type CsI photocathodes in vacuum. They claimed that the increase might be due to fact that for higher angles photoelectrons are produced nearer to the surface and so escape more easily. These results are not in agreement with the ones obtained by Miné et al.[17] in 1995 who measured the effect of incidence angle in the quantum efficiency of CsI photocathodes in vacuum. Their results showed a decrease of the quantum efficiency with the increase of the incidence angle. As we can see in **Figure 2.8 b)** they got up to a 30% decrease for a  $55^\circ$  incidence angle compared with perpendicular incidence, depending on the wavelength of the incident light. In their conclusions they refer that their results are in disagreement with the ones obtained by

Lopes and Conde. In 1999 Tremsin and Siegmund [18] measured this variation for angles up to  $\pm 55^\circ$  in the spectral range of 25-115 nm. Their results are shown in **Figure 2.8 c)**. They claim that their results are in accordance with a theoretical model proposed by Fraser [19] which is based on the absorption and escape length of photoelectrons.

All these are result obtained in vacuum. No data was found in the literature of this kind of measurement when the photocathode is placed in a gaseous atmosphere.

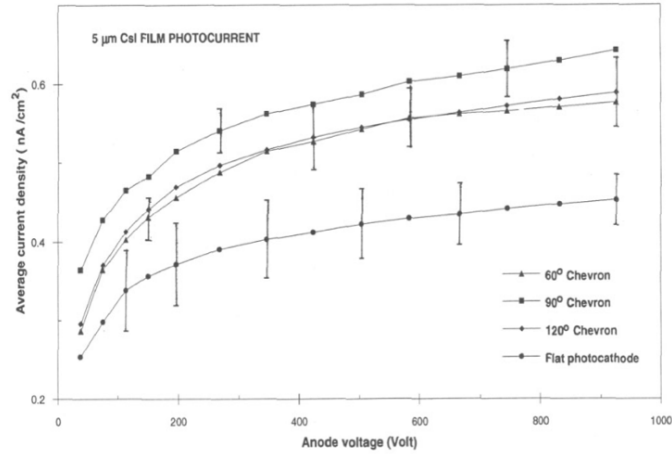


Fig. 2. — Average photocurrent density of a 5  $\mu\text{m}$  CsI film as a function of the anode voltage for flat and chevron photocathodes

a)

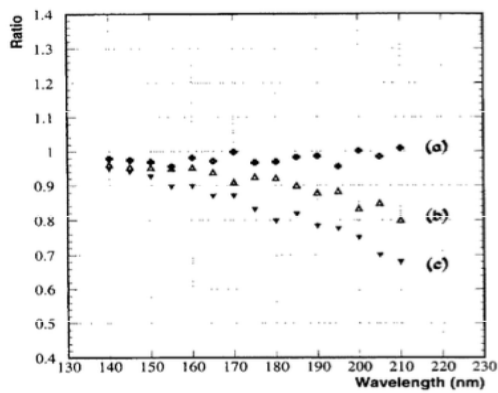
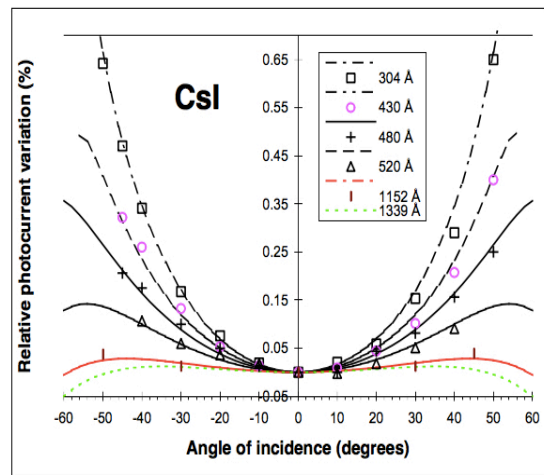


Fig. 2. Ratio of the QE of each cone to that of a flat photocathode manufactured in the same patch. A monotonic loss of QE with wavelength is observed. The values of the angle of incidence ( $\theta$ ) are: (a)  $15^\circ$ , (b)  $45^\circ$ , (c)  $55^\circ$ .

b)



c)

Figure 2. 8 - Results obtained by a) Lopes and Conde (1993); b) Miné et al. (1995); c) Tremsin and Siegmund (1999)

# 3. Experimental System

In order to conduct this study, an experimental system had to be designed and built. This task was performed taking into account that:

- the system must withstand high pressures up to 10 bar
- the system should allow an angle variation device

## 3.1 Operation Principle

The design used in [8] was the starting point, so our design is quite similar to it. The principle of operation is to measure the current produced when the emitted photoelectrons are collected. This is, the photocathode is irradiated by a constant fixed beam of collimated light, and when the photons hit the photocathode it produces photoelectrons. The photocathode is negatively polarized, while a collection grid in front of it is at ground potential, this drives the photoelectrons towards the grid, that grid is connected to an electrometer that measures the photocurrent produced. The photocathode stage (both photocathode and the grid) are connected to a linear motion feedthrough that allows their rotation to change the incidence angle of the beam of light in the photocathode.

This design allows us to change a wide range of parameters: the reduced electric field applied; the atmosphere inside the detector (changing the gas/mixture or the pressure); the incidence angle and the photocathode (photocathode material or substrate)

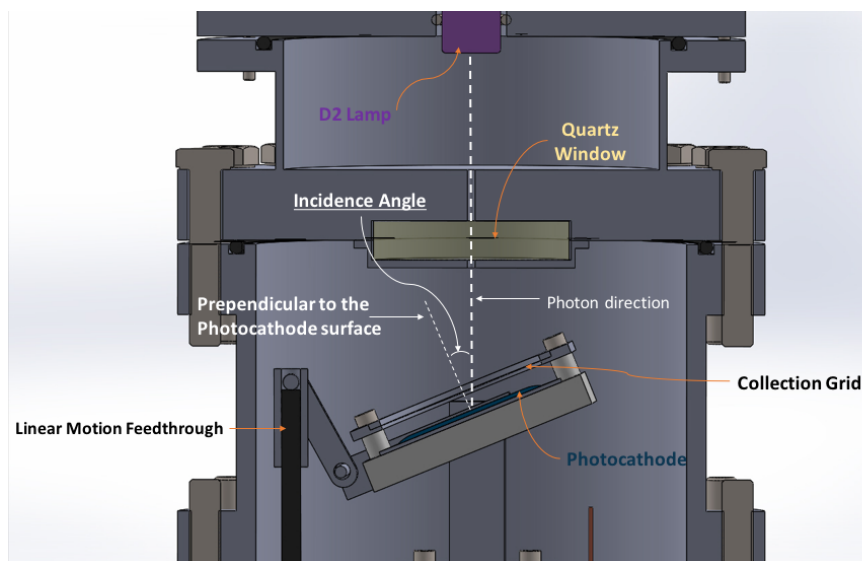


Figure 3. 1 - Schematic of the operational principle of the experimental system

### 3.2 Experimental setup

The starting point for our experimental setup was the photon source and, since a Deuterium Lamp (HAMAMATSU L2D2 L7296-50) was available and we decided to use it.

Regarding the photon source, it has a spectral distribution that can be seen in the **Figure 3.2 a)** [20]. This distribution includes two main limitations: firstly, the fact that it is a fixed spectral distribution, so to make a spectral analysis of the quantum efficiency, we would have to use filters; secondly, it is barely coincident with the known spectral response of the Quantum Efficiency of the CsI, and where the coincidence occurs ( $\sim 200 \text{ nm}$ ) the Q. E. of the CsI is very low (5% and below), as can be observed in **Figure 3.2 b)** taken from [12].

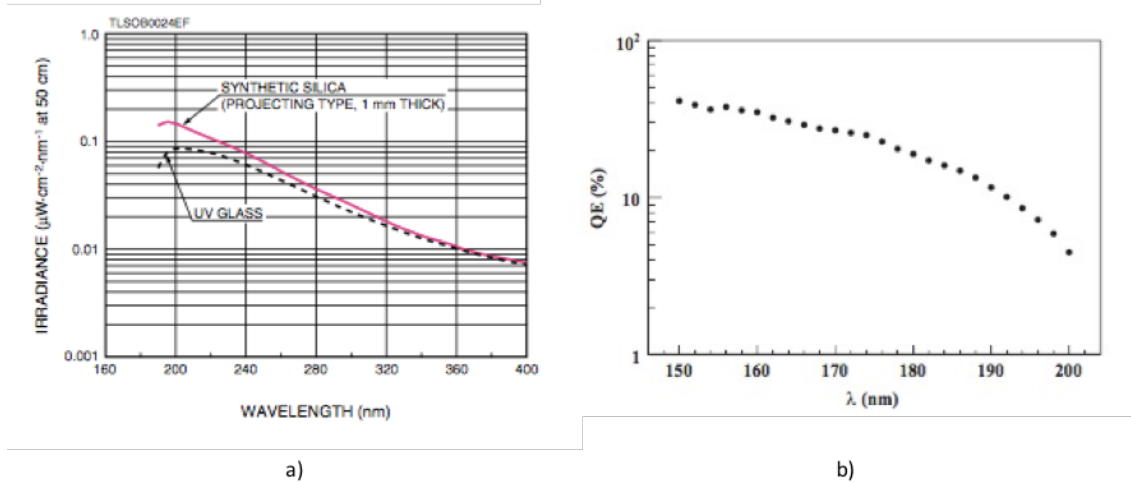


Figure 3. 2 - a) Spectral distribution of the Deuterium Lamp [20]; b) Spectral Responce of CsI photocathodes [12]

Since this lamp was for vacuum use only and it cannot bear high pressures, the solution was to divide the system into two chambers: one at vacuum in contact with the lamp, and one at high pressure for the measurement of the quantum efficiency itself.

The two chambers were separated by a quartz window (Heraeus Suprasil® 312), 1cm thick and 5 cm in diameter, that can withstand, using the formula from [21], in the worst case scenario, a pressure difference,  $\Delta P$ , of almost 20 atm, since

$$\Delta P = \left(\frac{2t}{A}\right)^2 \cdot \frac{S_F}{K \cdot f_s} = \left(\frac{2 \cdot 1}{5}\right)^2 \cdot \frac{60}{1,25 \cdot 4} = 1,92 \text{ MPa} = 19,2 \text{ bar}$$

where  $t$  = thickness of the window = 1 cm;



$A$  = unsupported aperture diameter = 5cm (worst case  $A$  = diameter of the window);

$S_F$  = Minimum Fracture Strength = 60 MPa (for fused silica, which is the window material);

$K$  = support constant = 1,25(value of the worst case, window is unclamped);

$f_s$  = safety factor = 4 (typically);

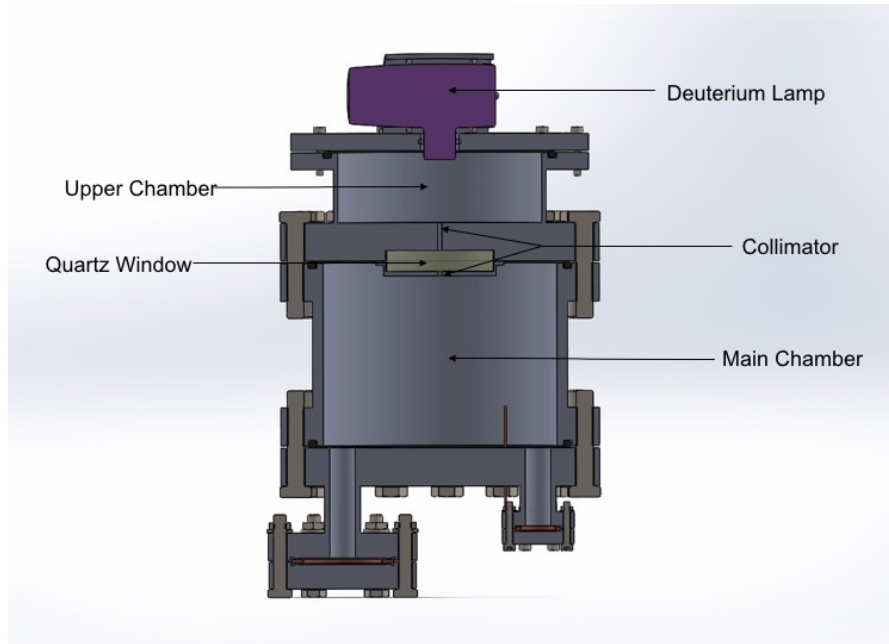


Figure 3. 3 - Schematic of the experimental system designed in Solidworks

The upper chamber should stay in vacuum to avoid photon absorption by the air. In fact, it was noticed that the presence of air in this chamber was harmful for our signal due to the photon absorption by it.

The separation region between chambers was also used to collimate the photon beam emitted by the lamp into a straight beam that will travel through the main chamber and hit the photocathode.

Since the main chamber is supposed to be working at a maximum pressure of 10 bar, it was designed to withstand up to 20 bar, for safety reasons. In **Figure 3.4** we can see a simulation run on Solidworks for the main chamber, where it is represented the chamber deformation due to the pressure inside. This simulation was made for a pressure inside the chamber of 20 bar and the deformation is correlated with the stress experienced as we can read in the figure. We can see that the maximum displacement occurs in the region where the quartz window should be placed (in the simulation, for simplification

purposes, was considered a solid body of cast stainless steel), and it can also be seen that this maximum displacement is of the order of  $1,00 \times 10^{-2} mm$  which is almost negligible. We concluded that it should be safe to operate at 10 bar.

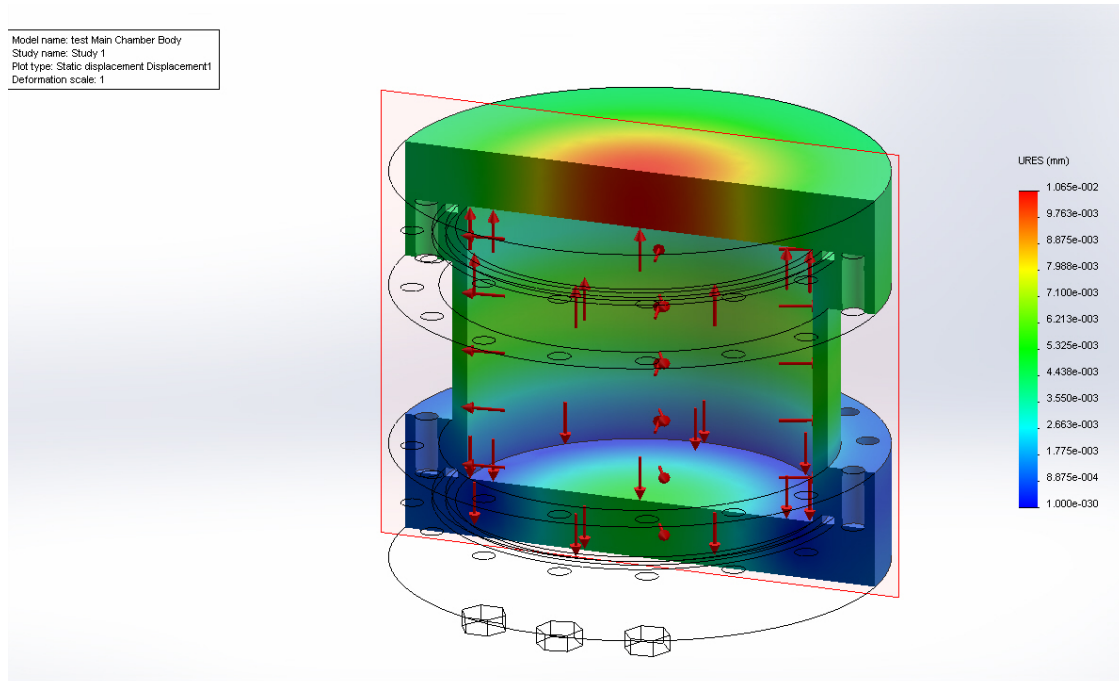


Figure 3. 4 - Simulation performed by Solidworks of the deformation that the main chamber of the experimental system at 20 bar

From the few studies in the literature concerning incidence angle dependence for photocathodes [17, 18], it could be seen that  $50^\circ$  is the common limit for these studies. Also this range of incidence angles covers most of the practical situations in the detectors that use photocathodes as energy converters, namely the case of the high pressure detector being developed at LIP Coimbra that motivated the study developed during this project time.

The solution found can be seen in the **Figure 3.5** and it is calibrated to sweep all the incidence angles between 0 and  $50^\circ$ .

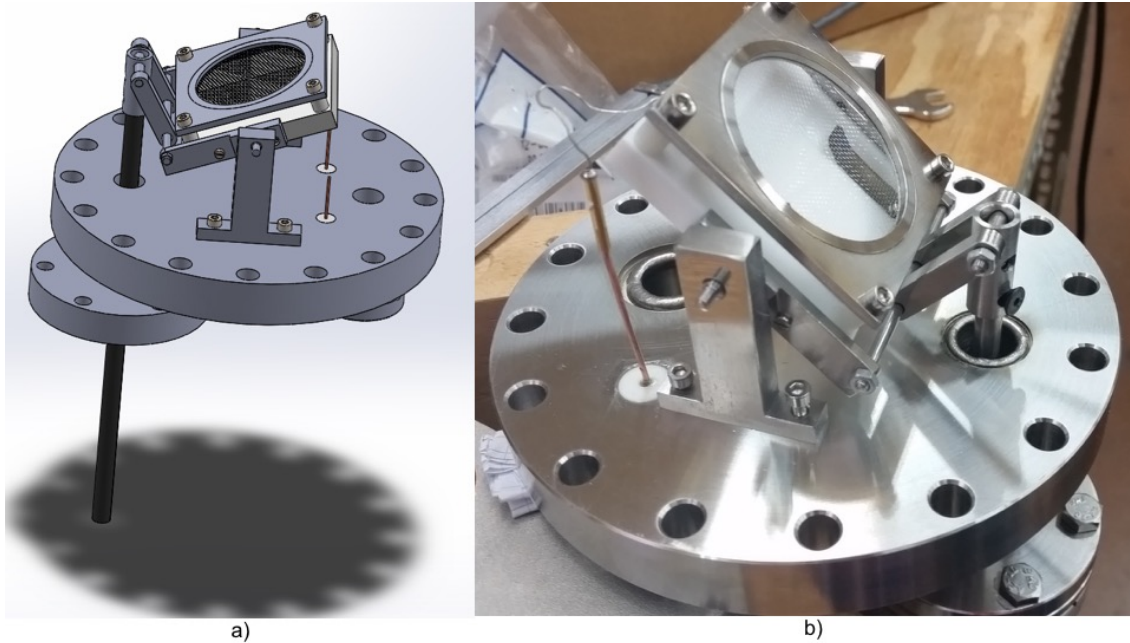


Figure 3. 5 - Angle variation device. a) Schematic designed in Solidworks; b) Photograph during the assembly of the experimental system

This angle variation is possible by the movement of a linear motion feedthrough that is connected to the photocathode and charge collecting grid support through a hinge. It was used a MDC 660050 feedthrough that has the drawback of being for vacuum purposes, but it was already available in the laboratory and one for high pressure had to be custom made, which would be very expensive.

As said before the electron production/collecting part was based on what is more commonly found in the literature, for this kind of studies.

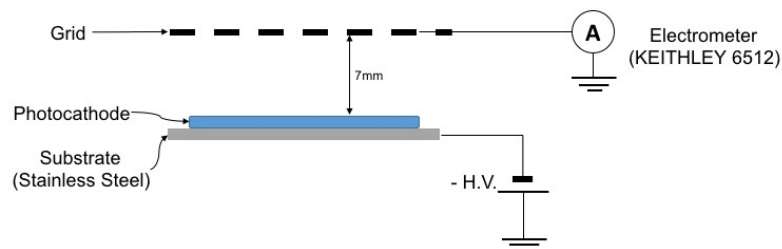


Figure 3. 6 - Schematic of the set up that allows the production and collection of the electrons

Here we can see that we have the CsI photocathode on a stainless steel substrate, 7mm bellow a metallic grid that will collect the photoelectrons emitted by the photocathode.

The photocathode substrate is maintained at a negative electric potential while the grid is at ground potential. This causes the photoelectrons emitted by the photocathode to be accelerated towards the grid. The grid is connected to an electrometer from KEITHLEY model 6512 that measures the photocurrent produced with a very high precision (4 significant figures).

We also had to correct for variation of the shadow of the grid with the incidence angle. From geometric considerations we could assemble the following table:

Angle	Shadow of the grid
0°	11,46%
5°	11,48%
10°	11,54%
15°	11,64%
20°	11,79%
25°	11,99%
30°	12,26%
35°	12,60%
40°	13,03%
45°	13,57%
50°	14,27%

*Table 1 - Shadow of the grid for different photon incidence angles*

### **3.3 Vacuum and Gas Insertion Line**

The experimental system described is included in a vacuum system (that controls the vacuum and the flux of gases in and out of the chambers).

**Figure 3.7** shows a schematic of this system and of the chamber used in the experimental measurements.

The vacuum system is composed by a turbomolecular pump (Leybold TurboV AC 151) backed by a rotary pump (Varian DS 302) and two vacuum meters, a thermocouple (Varian 0531) and a cold cathode gauge tube (Varian 525), placed at the entry of the turbomolecular pump and controlled by a pressure gauge controller (Varian SenTorr CC2

L91213021000). The ultimate vacuum attainable by this system is around  $5 \times 10^{-8}$  Torr at the head of the pump.

Nevertheless, due to the complexity of the vacuum line and the fact that the majority of the tubes that lead to the main chamber are very thin tubes (7 mm in diameter), with a very low vacuum conductivity[ref], the vacuum in the chamber is some orders of magnitude higher. The conductivity of the tubes was estimated and from it, we calculated the vacuum level at the entry of the turbomolecular pump (where the vacuum gauges are placed) to be lower than the level at the entry of the main chamber by a factor of  $\sim 10^{-3}$ . This is of course only an estimation and the real vacuum level inside the main chamber is unknown. This limitation excludes the possibility to study under vacuum conditions.

The same problem happens with the vacuum in the upper chamber. This means that, since the vacuum level in the upper chamber is not known precisely, the photon absorption by residual air molecules is also unknown. Hence, an absolute measurement of the extraction efficiency is difficult to be made with this experimental system.

The gas is inserted in the system through a gas vessel connected to the vacuum line system through a pressure gauge. A recovery vessel is also available to recover the gas between fillings in order to minimize the waste of gas. All these elements are connected to the main chamber through valves, with the purpose of making possible the isolation of different parts of the system.

Considering the main chamber circuit, there is parallel to the main chamber, and permanently connected to it, a gas purification tube with getters (SAES® St 707) to purify the gas in the main chamber. These getters are small pieces of a compound (V,Zr,Fe) that absorbs some molecular impurities (H<sub>2</sub>, N<sub>2</sub>, H<sub>2</sub>O, CO<sub>2</sub>) but doesn't absorb inert gases. These small pieces have a protective cover that has to be removed the first time it is used. This is done by heating them, in their first use, to 450°C, under vacuum, so the protective cover evaporates. After that, the getters need to be protected from air so that their absorption capacity isn't lost due to saturation. The absorption capacity can be controlled by the temperature of the "getters". They were operated at 150° which is a compromise between the maximization of their absorption capacity and their lifetime. [22, 23]

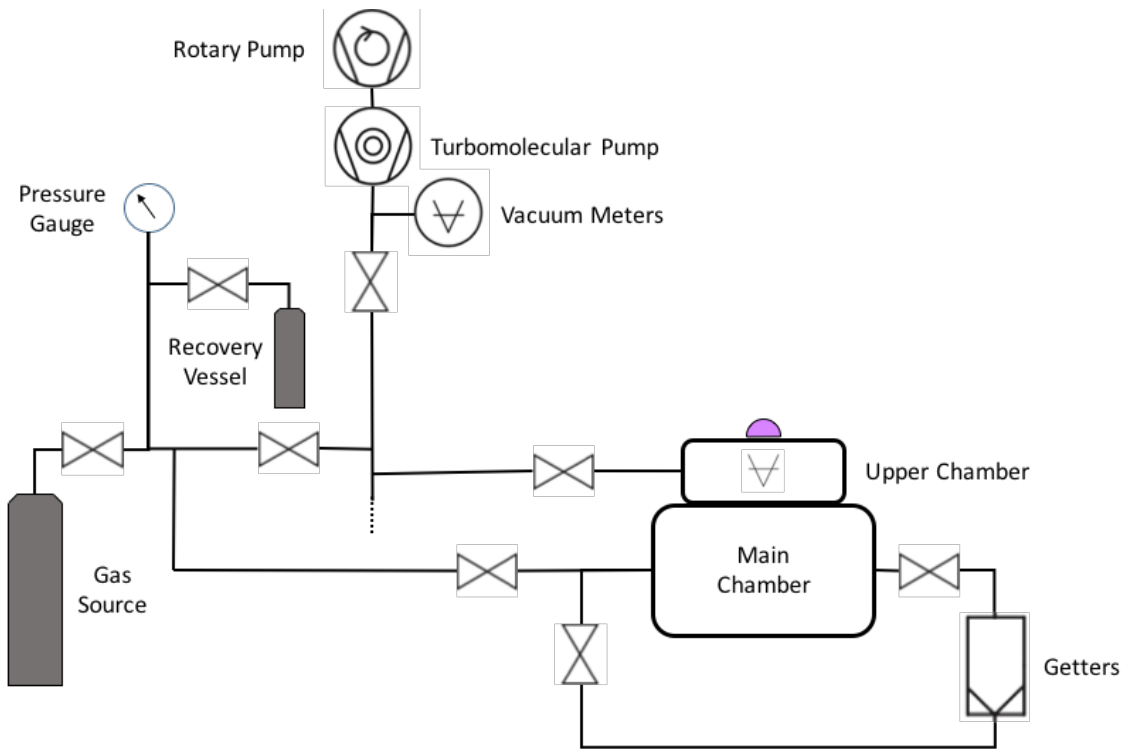


Figure 3. 7 - Schematic of the gas and vacuum line

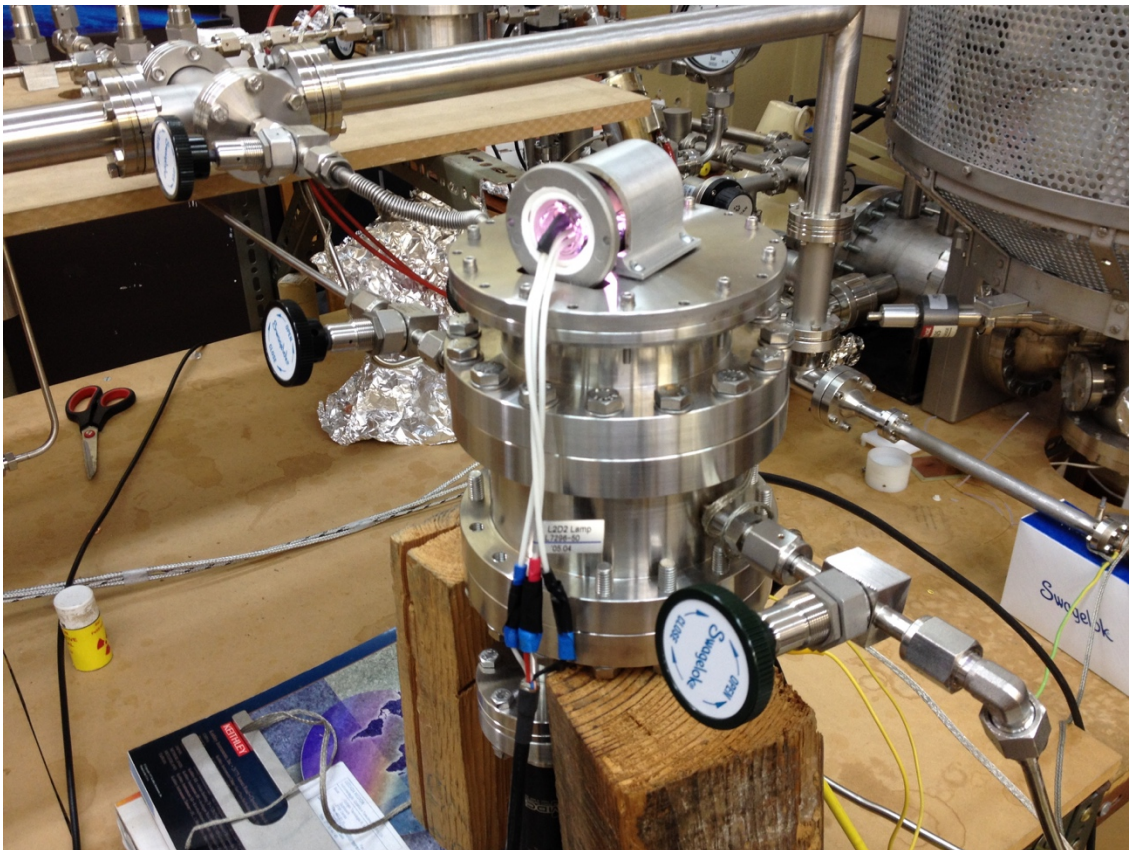


Figure 3. 8 - Photograph of the experimental system



### **3.4 CsI photocathode**

It was decided that the photocathode studied was going to be a Caesium Iodide (CsI) reflective photocathode. This choice was due to the fact that CsI photocathodes are the most widely used in gas detectors, hence the most interesting to study. Another reason was its stability after some minutes of exposure to air, in fact to the water molecules present in the air, that simplifies the processes of transport and assembly in the experimental setup, when compared to other photocathodes (namely CsTe).

Concerning reflective photocathodes, the substrate where they are deposited are an important factor regarding their quantum efficiency [24]. In this study the substrate chosen was a stainless steel plate.

The CsI film was evaporated in the stainless steel plate under a high vacuum environment ( $1,8 \times 10^{-5}$  mbar). It was used a piece of CsI in the crystal form, that was placed in a metallic boat shaped holder. When a high electric current went through the holder, the crystal melted and evaporated. It was deposited at a rate of  $\sim 20$  kÅ / minute until it reached a thickness of 568 nm.

After the film deposition, in order to transport the photocathode to the chamber it was placed in a box filled with nitrogen in order to minimize the exposure to water molecules during this transport. During this process we can estimate that the photocathode was exposed to air about 1 to 2 minutes.



a)



b)

Figure 3. 9 - a) Evaporation Plant; b) CsI crystals placed in the boat shaped holder

## 4. Methodology

The first time an experiment is made the results are often too crude. This leads to a process of refinement of the technique and method used in order to get what might be acceptable as a reliable description of the events in study.

That process happened in this study too. What, at the beginning, was viewed as almost as simple as measuring an electric current, turned out to converge into a more complex and time consuming process that I shall describe.

### 4.1 General description

As already mentioned, the main purpose of this work was to collect and measure the current produced by the photoelectrons emitted from the photocathode and to obtain a value for the extraction efficiency of the photocathode, for different photon incidence angles, different gas pressures, and reduced electric field.

Nevertheless, a process that was viewed as a simple measurement of an electric current, turned out to converge into a more complex and time consuming process that will be now described.

After the chamber was assembled and tested for vacuum we started the measurements, confirming that with the lamp turned on the current read in the electrometer had a value of the order of magnitude expected and was measurable with the electrometer used.

The first measurements began with the chamber under vacuum (at  $\sim 5 \times 10^{-6}$  Torr at the head of the pump and an electric field applied  $E = \sim 28,6 \text{ V} \cdot \text{mm}^{-1}$ ) and it was observed that the current signal measured showed a decreasing behaviour with time that was hard to explain. Several tests were performed changing the possible variables that can be controlled within this system such as the vacuum level and the potential applied to the photocathode. One variable that could be associated to this behaviour was the irradiation time of the photocathode. **Figure 4.1** shows the plotting of the current measured values in function of time where this behaviour can be observed.

It was also observed that the measured value of the current was dependent of the vacuum level on the upper chamber. This is expected since it is known that the UV photons are absorbed in air and can also be explained by the fact that the lamp starts to heat considerably after about 20 minutes of use, until it reaches a temperature around



90°C and, therefore, heats the whole upper chamber body, and the top half of the main chamber body. This may originate an increase in the outgassing and therefore an increase of the pressure in the upper chamber.

In **Figure 4.1** there are two plots of the current dependence with time, the orange points represent a series of values taken with the upper chamber being continuously pumped down, while the blue ones represent a series of values taken with the upper chamber pumped and closed. We can see that in the case when the upper chamber is being continuously evacuated the decrease in the current stabilizes (stops decreasing, or decreases with a very small slope) after about 40 min, which doesn't happen when the pressure is higher in the upper chamber.

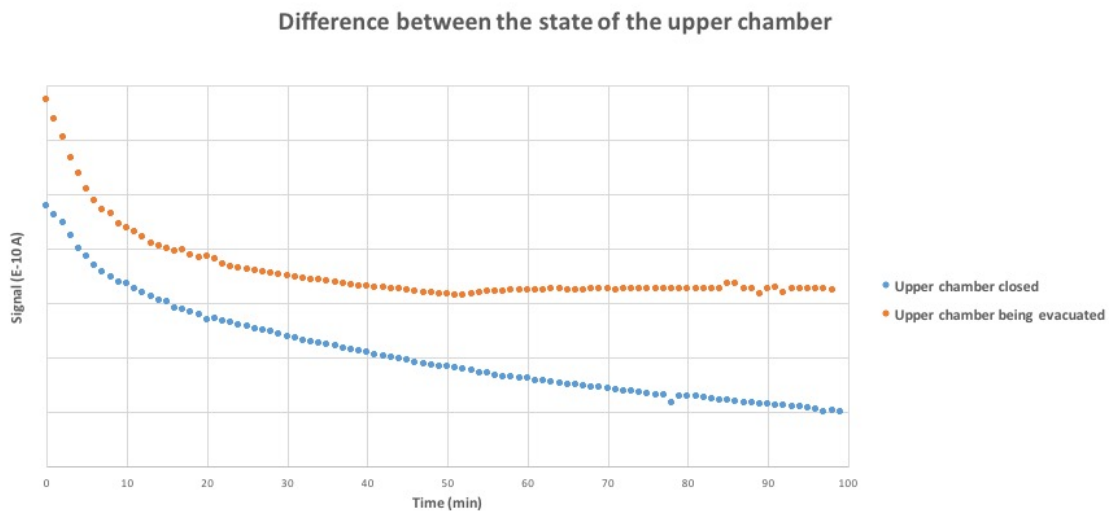


Figure 4. 1 - Behaviour of the signal produced by the photocathode over time. At orange, with the upper chamber being evacuated. At blue, with the upper chamber closed, after being evacuated

The fact that in our system the pressure in the upper chamber was not monitored and that the photon flux entering the main chamber is dependent on this residual pressure, only relative measurements of the extraction efficiency of the photocathode were performed. To take into account the limitations described, before any data acquisition experiment, the value of the signal was recorded each minute for a period of 100 minutes. After data acquisition, the same was done over 20 minutes, and a trend line was adjusted to these data. This trend line was then considered as the reference for the measured value, as it can be seen in **Figure 4.2**.

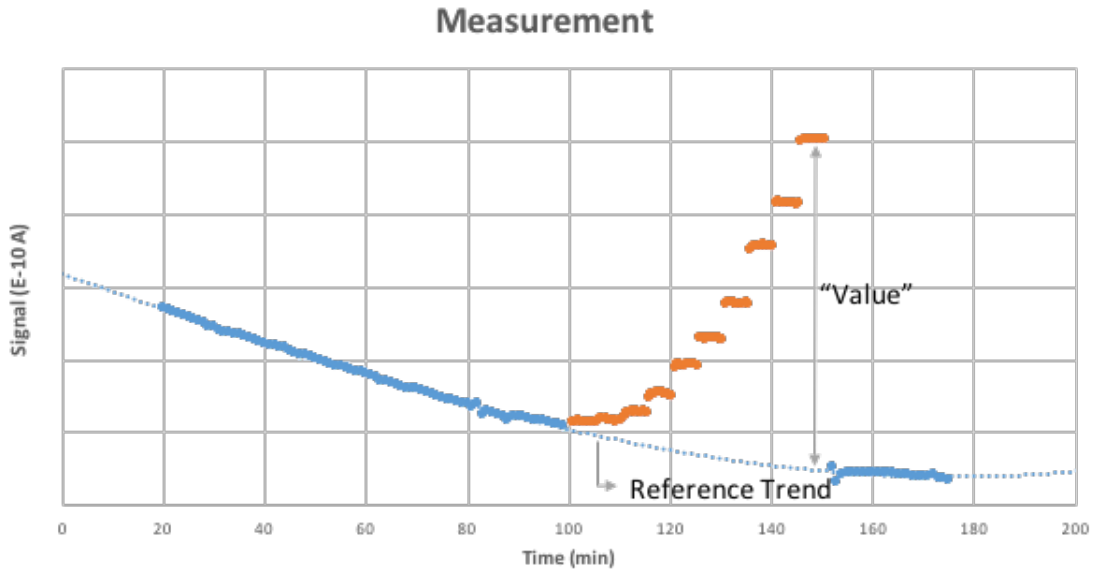


Figure 4. 2 - Schematic of how a measurement was performed

**Figure 4.2** illustrates the whole process of taking a measurement of the Relative Extraction Efficiency (REE), that lasts for about 3 hours.

When changing the angle of incidence of the photon beam, we started with 100 minutes for the stabilization of the current at  $0^\circ$  (horizontal position of the photocathode) that is the chosen as the reference. After this we started to vary the angle. For each angle 10 measurements were taken in 5 minutes. Comparing each point with the reference trend we get the current value for that angle, and the weighted mean of the 10 values for each incidence angle will give the final value for that angle. The uncertainties associated with each final value will be discussed in more detail in **section 4.3**.

The measurement just described was also performed for different values of reduced electric field ( $E/p$ ) to study the impact of this parameter in the variation of the REE with the photon incidence angle.

Also, in order to study in more detail, the variation of REE with  $E/p$  above the photocathode, a second type of measurement was performed, in which the angle was kept constant in each measurement and the dependence of the REE with  $E/p$  was studied. This measurement was performed in the way described before, taking for the reference value a small value for  $E/p$ .

Another thing that is important to mention, is that in the study of the dependence of the REE with the incidence angle what is presented is the percentage of increase of this value, with

$$\%(\Delta\text{REE}) = \frac{\text{Value} - \text{Value}(0^{\text{e}})}{\text{Value}(0^{\text{e}})} \times 100.$$

For the measurement of the dependence of the REE with the E/p, since there is a strong increase with E/p, the expression above can be reduced to:

$$\Delta\text{REE} = \frac{\text{Value} - \text{Ref.Value}}{\text{Ref.Value}} \approx \frac{\text{Value}}{\text{Ref.Value}}.$$

As mentioned in [11] for xenon the threshold for photon feedback is  $E/p \sim 1,5 \text{ V} \cdot \text{Torr}^{-1} \cdot \text{cm}^{-1}$ . Since for this work this effect is not desirable only reduced electric fields equal or bellow  $1 \text{ V} \cdot \text{Torr}^{-1} \cdot \text{cm}^{-1}$  were used.

## **4.2 Dark Current**

Defining dark current as the current measured in the electrometer when the lamp is turned off, this is one of the main aspects that can affect the current measurements, since these currents are of the order of  $10^{-10} \text{ A}$ . We believe that this dark current is due mainly to the ground fluctuations originated either by the surrounding instruments in the laboratory and from other parts of the building. To accurately take into account this factor, an uncertainty factor is introduced in the data analysis.

In order to quantify this uncertainty, values of the dark current were measured every hour for several periods during about 4 days and then the average of all these values was assumed to be the value of the dark current uncertainty,  $\sigma_{DC} = 0,0098 (\times 10^{-10} \text{ A})$ .

Nevertheless, we note that sometimes the dark current fluctuations had a much higher amplitude, which we believed was due to a source outside. Anyway, in these conditions, the measurements were not considered.

## **4.3 Uncertainty and Error Propagation**

We will now explain in more detail the method considered to find the uncertainty in the measured values, taking into account all the error sources referred to before.

Regarding the reference trend, its relative error is associated to the value of  $R^2$  given by the fitting. Hence, the values from that trend function have a corresponding uncertainty,  $\sigma_R$ .

Considering the value read in the electrometer, it is affected by the uncertainty of the electrometer and by the dark current fluctuations. The dark current uncertainty,  $\sigma_{DC}$ ,

was already explained in the previous section. The uncertainty of the electrometer,  $\sigma_E$ , is just the uncertainty of a digital instrument that corresponds to the last significant figure.

With the uncertainty of the individual values (designated by  $v$ ),  $\sigma_v$ , and considering that these effects are independent from each other, we obtain the uncertainty in the current values from the error propagation formula.

$$\sigma_x^2 = \sigma_u^2 \cdot \left(\frac{\partial x}{\partial u}\right)^2 + \sigma_v^2 \cdot \left(\frac{\partial x}{\partial v}\right)^2 + \dots$$

Hence, we obtain:

$$\sigma_V^2 = \sigma_M^2 \cdot \left(\frac{1}{Ref.}\right)^2 + \sigma_R^2 \cdot \left(-\frac{Mes.}{Ref.^2}\right)^2$$

where,

*Mes.* = Measured value in the electrometer

*Ref.* = Value of the reference

$$\sigma_M = \text{uncertainty of Mes.}, \quad \text{and } \sigma_M^2 = \sigma_e^2 + \sigma_{DC}^2$$

The final value, as mentioned in **section 4.1**, was obtained by averaging the several measurements made for each situation. Since these values have different associated uncertainties, we have to calculate its weighted mean, which is given by [25]:

$$Final\ value = \frac{\sum \frac{v_i}{\sigma_{v_i}^2}}{\sum \frac{1}{\sigma_{v_i}^2}}$$

with an uncertainty given by [25]:

$$\sigma_{final} = \frac{1}{\sum \frac{1}{\sigma_{v_i}^2}}$$

This corresponds to the final uncertainty presented for all the values in this study.

# 5. Experimental Results and Discussion

The purpose of this study was to study the variation of the REE of photocathodes with the incidence angle for photocathodes immersed in a gaseous atmosphere.

The study was performed with CsI as the photocathode and in a gaseous atmosphere of pure Xenon for different pressures:  $\frac{1}{2}$ , 1, 2, 3, 4 and 5 bar.

In the studies presented in this chapter we study the behaviour of the REE with the incidence angle (in **section 5.1**) or with the E/p (in **section 5.2**) and the influence of the other parameters (pressure in both studies, but E/p in **section 5.1** and incidence angle in **section 5.2**) in this behaviour, as explained in the previous chapter. For instance, when we say in **section 5.1**, that the variation of the REE with the angle is not dependent on the E/p, we are not talking about REE itself but the behavior that REE presents when we change the incidence angle. And the same is applied for the study in **section 5.2**.

This is important to clarify since it might, easily, lead to confusion.

## **5.1 REE variation with the incidence angle for constant E/p**

For each pressure of Xe we measured the REE for incidence angles between  $0^\circ$  and  $50^\circ$ , in steps of  $5^\circ$ . This was done for different values of reduced electric fields (E/p) to study the dependence of the variation of REE with the photon incidence angle on this parameter.

**Figures 5.1 to 5.6** show the results obtained. The points are hidden showing only the error bars, that were determined as already explained in **section 4.3**. Each line represents a measurement at a characteristic E/p. The line is only guides to the eye.

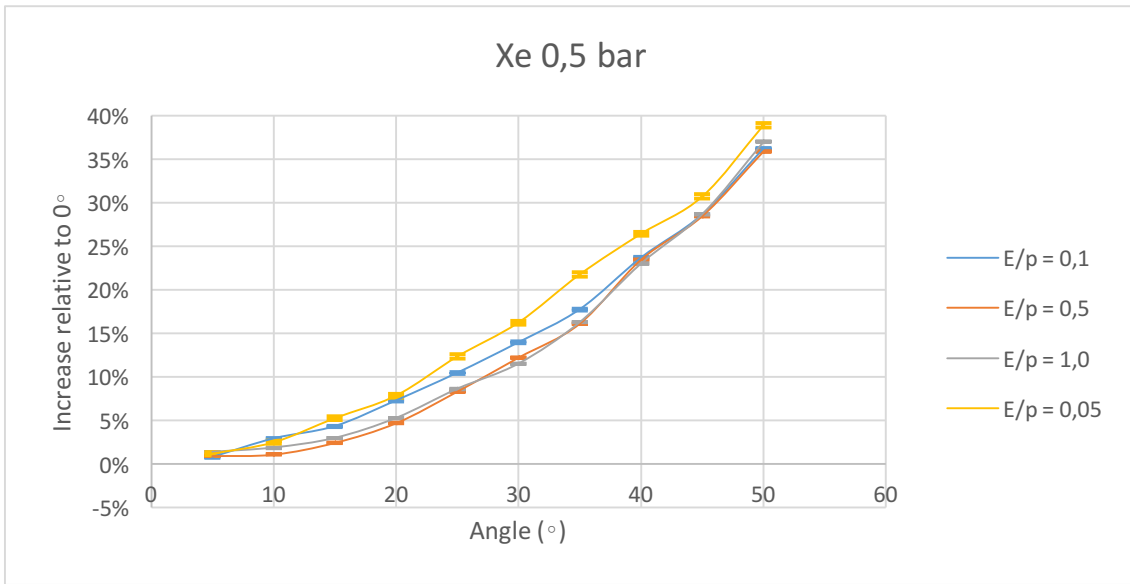


Figure 5. 1 - Obtained results for REE variation with the incidence angle for different E/p values at 0,5 bar of Xe. Values are relative to the 0° incidence angle

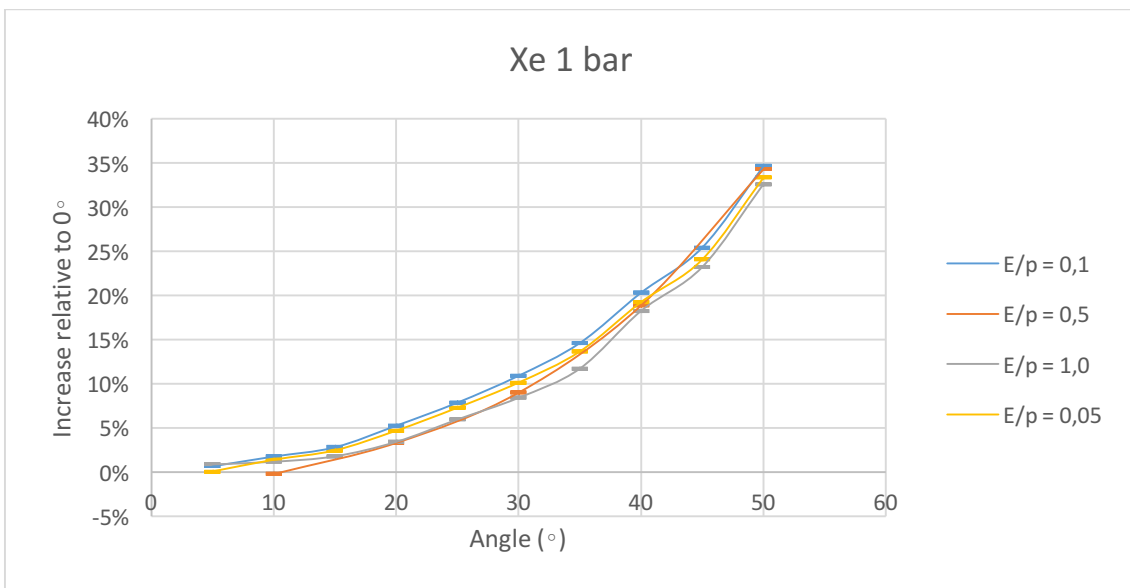


Figure 5. 2 - Obtained results for REE variation with the incidence angle for different E/p values at 1 bar of Xe. Values are relative to the 0° incidence angle

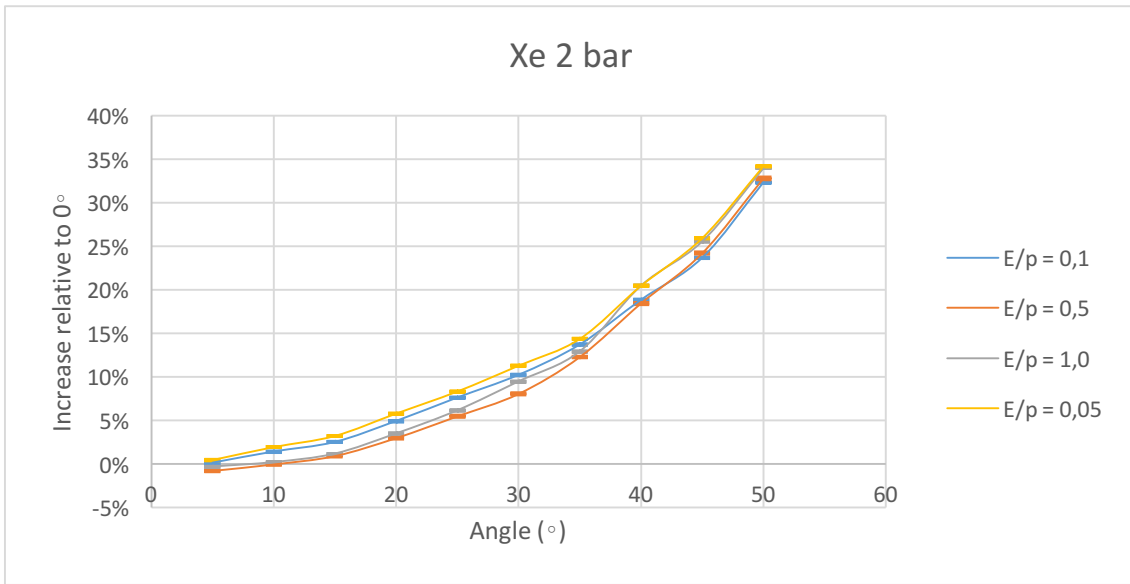


Figure 5. 3 - Obtained results for REE variation with the incidence angle for different E/p values at 2 bar of Xe. Values are relative to the 0° incidence angle.

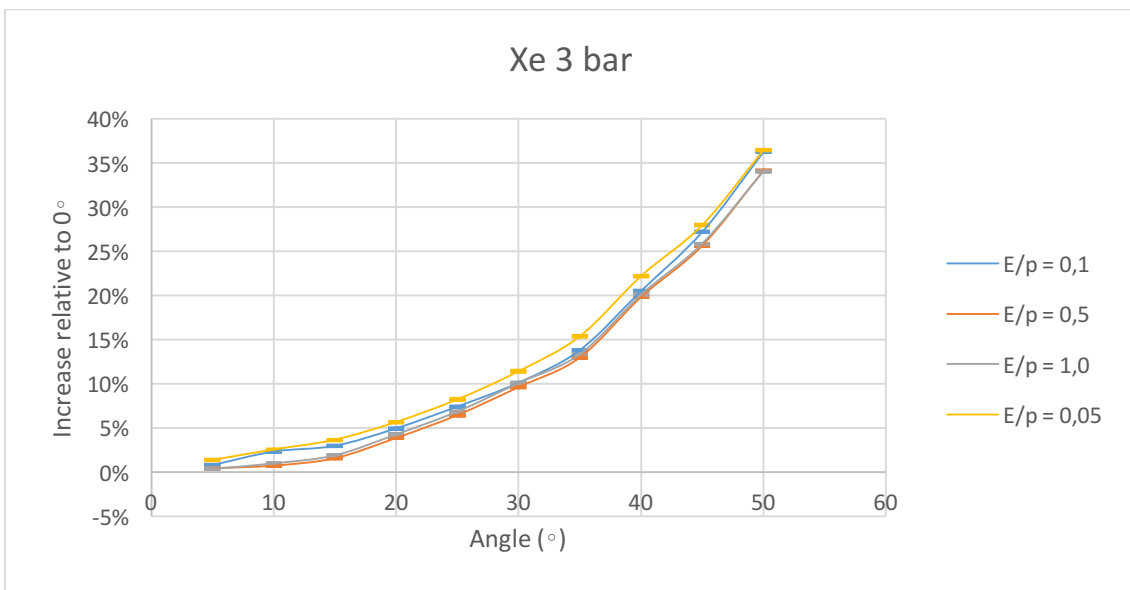


Figure 5. 4 - Obtained results for REE variation with the incidence angle for different E/p values at 3 bar of Xe. Values are relative to the 0° incidence angle.

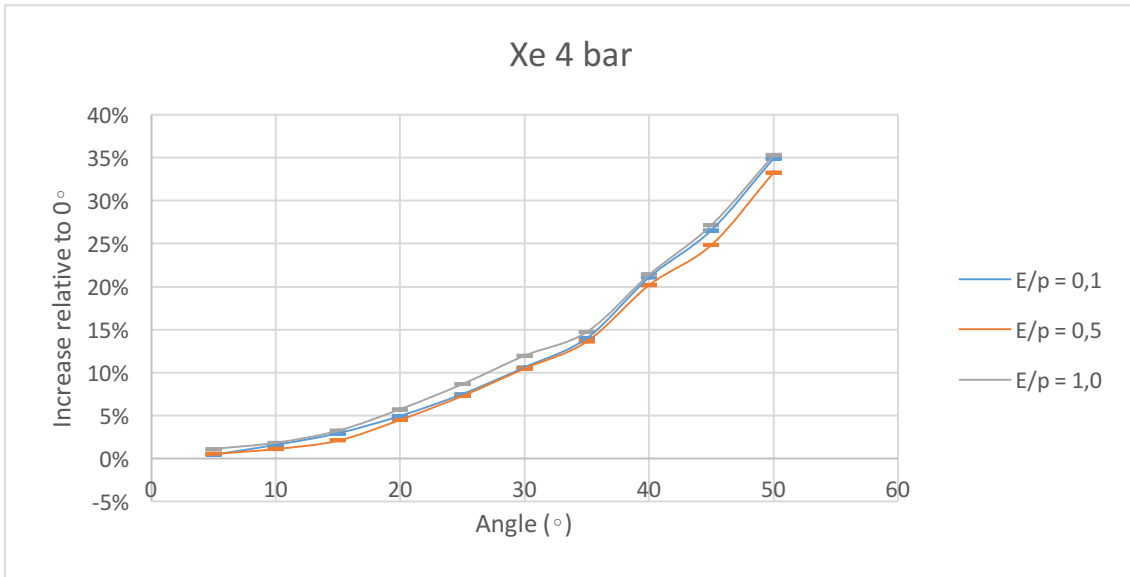


Figure 5. 5 - Obtained results for REE variation with the incidence angle for different E/p values at 4 bar of Xe. Values are relative to the 0° incidence angle

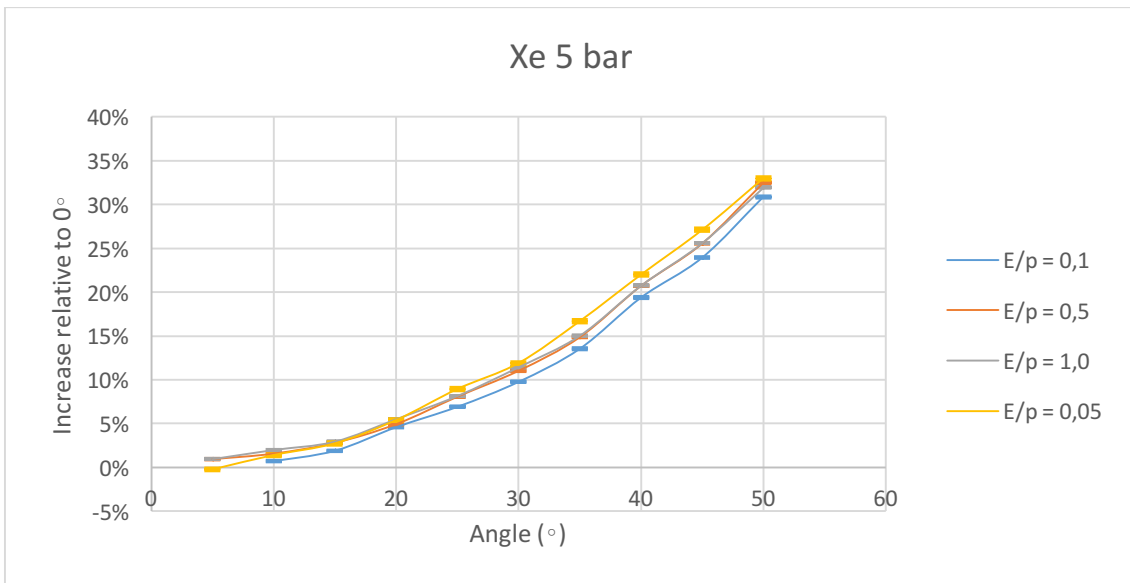


Figure 5. 6 - Obtained results for REE variation with the incidence angle for different E/p values at 5 bar of Xe. Values are relative to the 0° incidence angle

From these results we can see that for each Xe pressure the dependence of the REE with incidence angle always shows the same behaviour. In fact, the plot of the values of the REE have always the same shape and the values obtained for each angle relative to the 0° angle for the same conditions are consistent with the obtained for other pressures. For instance, at 50° incidence angle, all the measurements show an increase of ~35% of the REE, when compared to the 0° incidence angle.



So, the behaviour of REE with the incidence angle seems to be independent of both the pressure of the gas and the reduced electric field,  $E/p$ . This means that the number of collisions with Xe atoms and the energy added to the electrons after escaping from the photocathode are not relevant factors when considering the dependence of the REE with the incident angle of the photons.

This indicates that the dependence of photoemission of the photocathode with the incidence angle is related only to factors of the photocathode itself, in accordance with the studies of Lopes and Conde [16] and Tremsin and Siegmund [18]. Both authors attributed their results to the features of the photocathode, as already mentioned in **section 2.7**. One of the features is the depth at which the photon interaction with electrons of the material occurs and so with the depth at which photoelectrons are produced. Due to geometric reasons, as the incidence angle increases, electrons are produced closer to the surface, leading to lower losses of energy in the path towards the surface of the photocathode and so to a larger number of photoelectrons that can reach the surface with enough energy to escape from the material. This was suggested by Lopes and Conde, and this hypothesis is also compatible with Tremsin and Siegmund that suggest that the production depth depends on the light absorption of the photocathode material and is related to the escape length of the electrons produced.

Nevertheless, since we are talking about a reflective photocathode, the reflectivity of the substrate and the thickness of the photocathode might also have some influence on the results obtained. This arise from the description of the operation principle of reflective photocathodes (that was mentioned in **section 2.4**) and since the photocathodes quantum efficiency was found to be affected by the substrate [24].

## **5.2 REE variation with $E/p$ for a constant photon incidence angle<sup>2</sup>**

One of the most important parameters of operation with photocathodes is the reduced electric field applied above it, which sometimes limits its use in practical applications. In fact, an electric field is usually applied above the photocathode in order to drive the photoelectrons to a certain direction.

---

<sup>2</sup> In this section, the  $E/p$  units,  $V \cdot Torr^{-1} \cdot cm^{-1}$ , are hidden for simplification purposes.

For this reason, we thought that it would be interesting to study the dependence of the REE on the  $E/p$  for different incidence angles. We note once again that the reference is different for each curve and is the photocurrent measured for the  $E/p$  value considered as the reference. The reason for the choice of each reference  $E/p$  is explained below.

**Figures 5.7 to 5.12** show the results obtained for these measurements. Here again, the lines are only guides to the eye. And, in this study, each line corresponds to a measurement at a specific incidence angle.

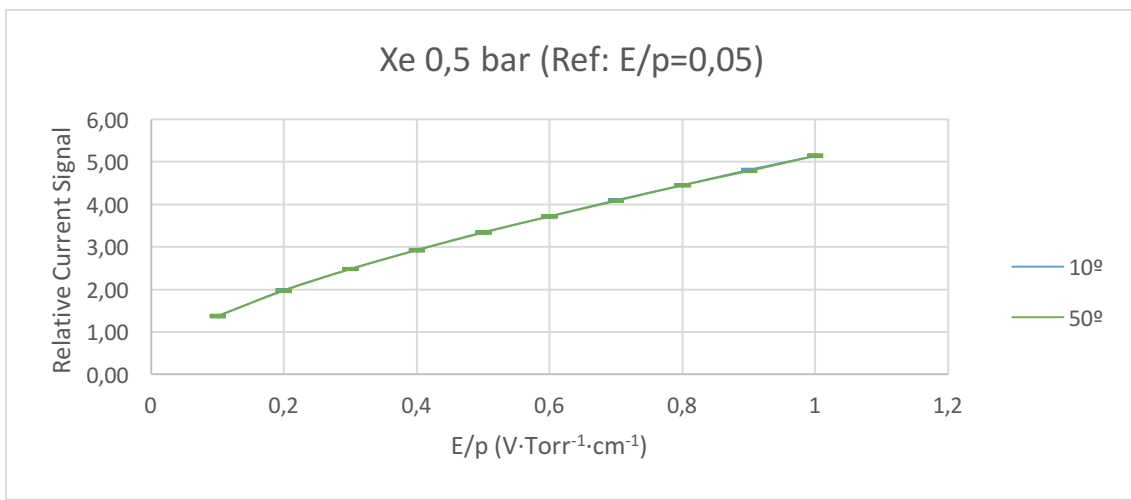


Figure 5. 7 - Obtained results for REE variation with  $E/p$  for a constant photon incidence angle at 0,5 bar of Xe. Here, the two measurements are coincident

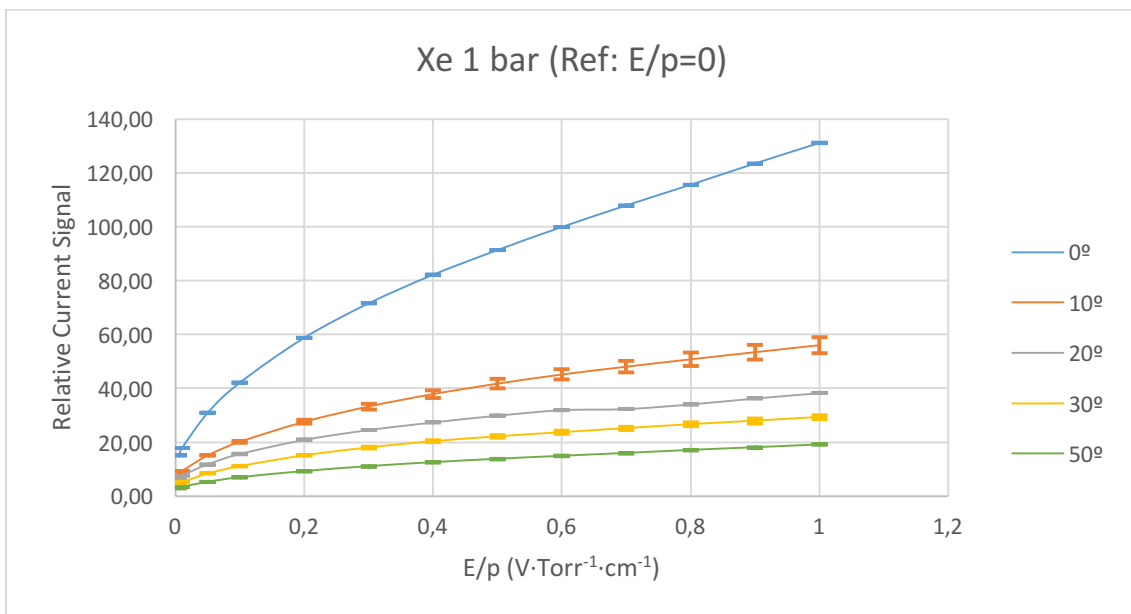


Figure 5. 8 - Obtained results for REE variation with  $E/p$  for a constant photon incidence angle at 1 bar of Xe

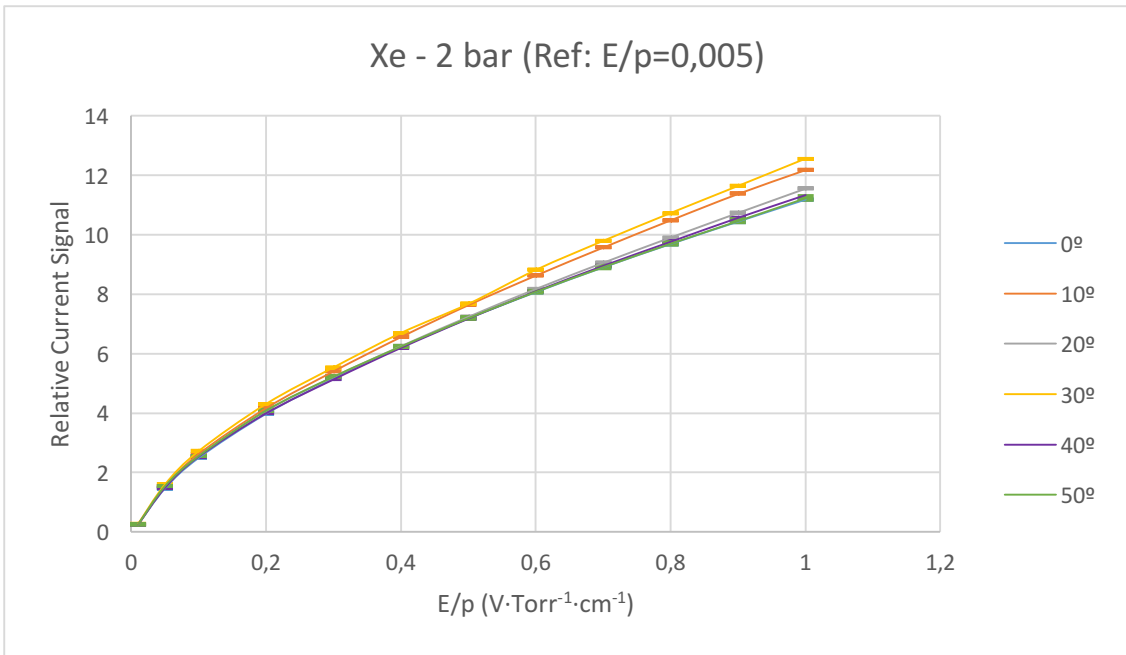


Figure 5. 9 - Obtained results for REE variation with E/p for a constant photon incidence angle at 2 bar of Xe

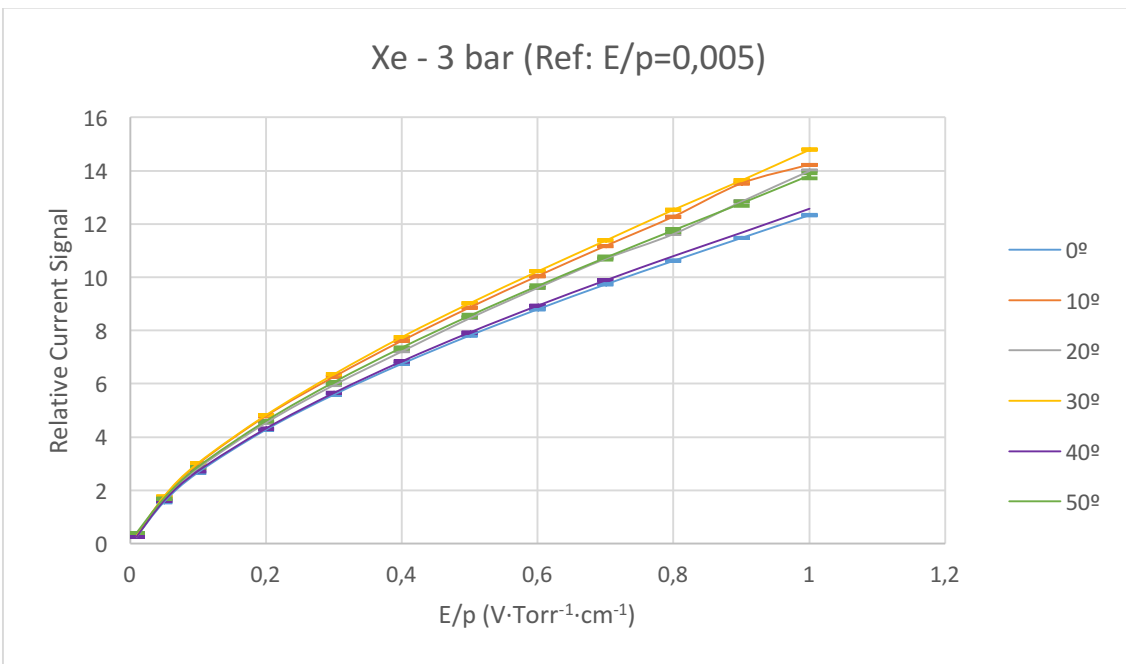


Figure 5. 10 - Obtained results for REE variation with E/p for a constant photon incidence angle at 3 bar of Xe

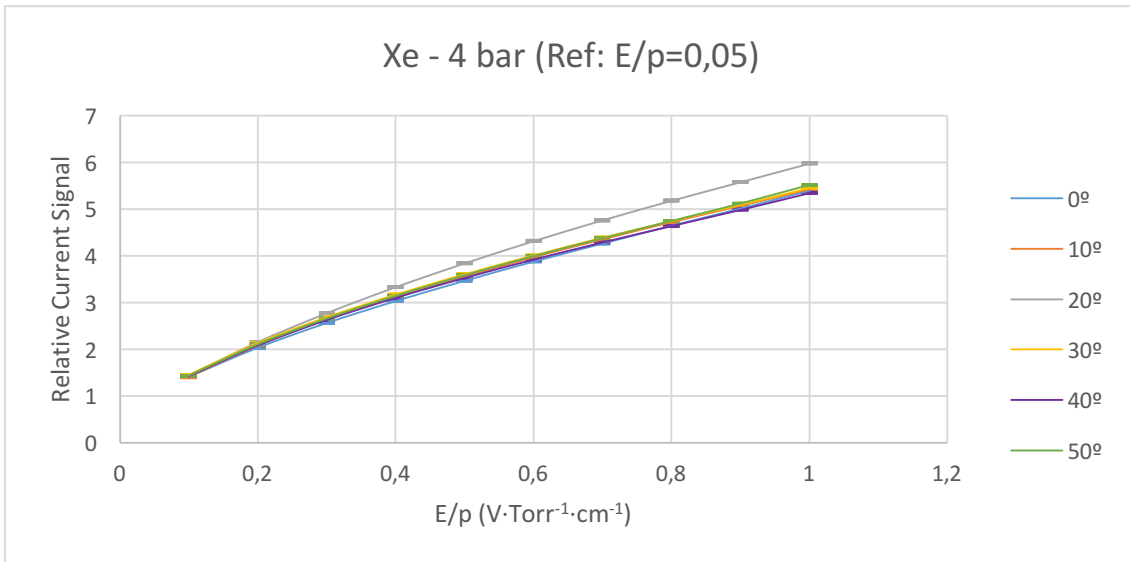


Figure 5. 11 - Obtained results for REE variation with E/p for a constant photon incidence angle at 4 bar of Xe

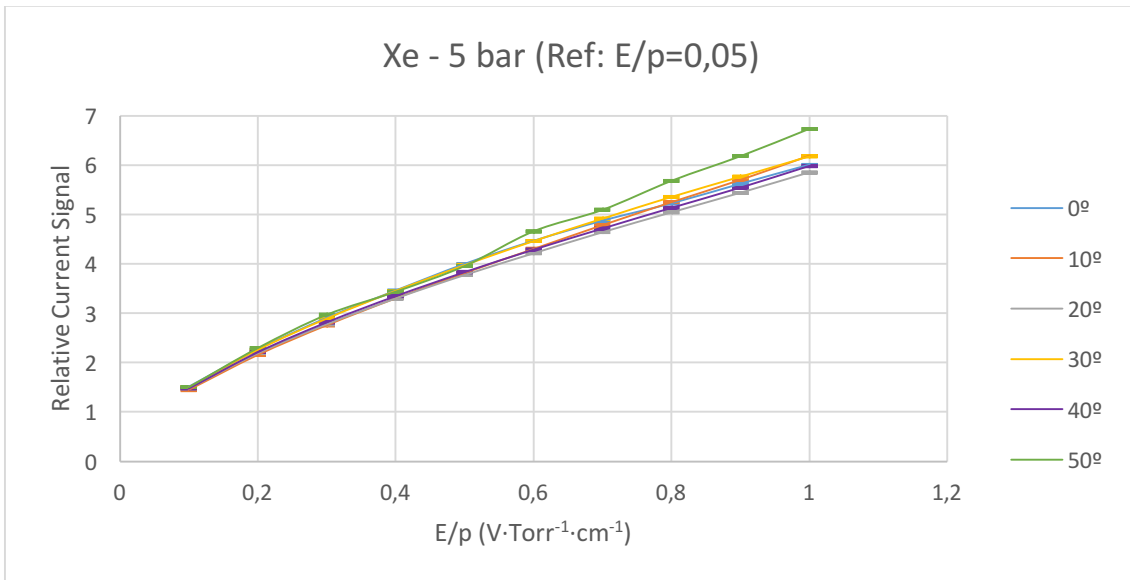


Figure 5. 12 - Obtained results for REE variation with E/p for a constant photon incidence angle at 5 bar of Xe

It can be observed that for all the pressures there is an increase in the obtained photocurrent from the reference E/p value to near  $1\text{Vcm}^{-1}\text{Torr}^{-1}$ , although for most pressures it seems that this increase does not depend on the incidence angle. The value of  $E/p=1\text{V}\cdot\text{Torr}^{-1}\cdot\text{cm}^{-1}$  was chosen as the upper limit since for values above this one, which is the Xe excitation threshold, it is expected photon feedback.

The main difference between the results obtained for the different pressures studied is the reference E/p that was adopted for each pressure. We will now explain briefly the reason for choosing these different E/p values.

For 1 bar pressure, it was noticed that there was no need to apply an electric field to have a photocurrent reading in the electrometer. This photocurrent was lower than the photocurrent obtained for the cases with  $E/p$  different the zero but it was enough to be read with accuracy, since it was considerably larger than the dark current, and the decreasing behaviour experienced before and illustrated in the **Figure 4.1** was also observable, this clearly meaning that for 1 bar pressure the photoelectrons emitted by the photocathode have enough energy to reach the collection grid.

So, we considered as the reference for the reduced electric field the value  $E/p=0$ .

For the other pressures studied, it was noticed that with no reduced electric field applied ( $E/p=0$ ) the current signal indistinguishable of the dark current, meaning that for pressures higher than 1 bar the emitted photoelectrons suffer collisions with the gas atoms and most of them are probably backscattered to the photocathode. For this reason they need some additional energy to be able to escape the photocathode surface and reach the grid.

So, values of a small  $E/p$ , chosen when the current read was at least two orders of magnitude higher than the dark current were taken as a reference for the other pressures.

This explains the difference between the results for 1 bar and the others.

In the 1 bar graph we can see that the higher the incidence angle, the lower the value of the REE. Nevertheless, this effect was not observable for other pressures, and we can conclude that the dependence of the REE with  $E/p$  does not change with the photon incidence angle. For this reason, the only thing that can explain this difference between the 1 bar behaviour and the behaviour for the other pressures is the difference in the reference value for  $E/p$ . Hence, the behaviour shown in the results for 1 bar is due to fact that the reference signal, this means the signal obtained with  $E/p=0$ , increases with the incidence angle, making the relative measure of extraction efficiency lower. In fact, since, as explained in the previous section, the higher the incidence angle the higher is the energy of the emitted photoelectrons, without any electric field applied the photoelectrons from higher incidence angles will have higher energy and originate a higher reference current. Therefore, when comparing the difference in the current signal for a certain  $E/p$  value with the  $E/p$  reference since the reference is higher we obtain a lower value for the REE.

For the other pressures, once we realised that for more than 1 bar  $E/p=0$  was not a good reference, we concluded that the reference needed to be replaced from  $E/p=0$  by another value.

This is expected, since for higher pressures there will be more gas atoms with which the photoelectrons can collide, thus, losing energy and eventually being backscattered to the photocathode and so not being able to reach the collection grid.

This is the reason why we found three different values of reference,  $E/p=0$  at 1 bar,  $E/p=0,005$  at 2 and 3 bar, and  $E/p=0,05$  at 4, 5 and 0,5 bar. The reference values for 2 and 3 bar differ from the ones for 4 and 5, because for these higher pressures those  $E/p$  values were not enough to have a photocurrent signal distinguishable from the dark current. This can be explained by the fact that for higher pressures the collisions with the gas atoms are more abundant and so the backscattering is more probable. For this reason for higher pressures, for the electrons to gain enough kinetic energy to surpass all the collisions they will suffer without being backscattered, a higher electric field must be applied. So, the reference value for  $E/p$  must be increased with the pressure.

The reason that the measurements at 0,5 bar were done with such a high reference for  $E/p$  is the fact that they were the last ones to be made and at this time the photocathode was already originating very small currents, since it had already had more than 300 hours of irradiation leading to a substantial aging effect, so we raised the value of the  $E/p$  reference to compensate this.

Also, for this pressure only two incidence angles were measured due to lack of time.

Despite these differences we can conclude that the dependence of REE with  $E/p$  does not change with the photon incidence angle, but increases with increasing  $E/p$  value for all incidence angles with the same trend line. This is also in agreement with the results obtained by Covita 2011 although a quantitative comparison is difficult since our measurements are relative.

Some deviations appear in the results, but we believe that this is due to the variation of the pressure in the upper chamber, like for example in the measurement for  $50^\circ$  at 5 bar that seems to be a little higher than the others. Cases like this were found to be correlated to the vacuum level of the upper chamber, as explained before. In fact, the heating of the deuterium lamp induces a raise in the outgassing in the upper chamber which raises the residual pressure there and reduces the light intensity that hits the photocathode. For this reason, we tried to perform the measurements with constant pumping on the upper chamber, and with time the outgassing tends to diminish and the residual pressure starts to drop. Thus, at the end of a set of measurements, when the photocurrent values for higher  $E/p$  are taken, if the residual pressure is still decreasing

and if it is at a lower level than it was when the first measurements of the set (for smaller  $E/p$ ) were taken, this results in a deviation of the curve in the region of the high  $E/p$ , for higher photocurrent values. When this happened, the measurement for the most obvious cases were excluded and an effort was made to take other measurements for the same pressure conditions in the upper chamber, despite these conditions being difficult to measure exactly.

### **5.3 Reproducibility**

Although the photocurrent measurements were quite reproducible, they were sometimes repeated over time to verify that according results were obtained. This happened most of the times and when it didn't happen a reason for the unexpected behaviour was usually found.

In the last measurements of the REE variation with  $E/p$  for constant incidence angle, some deviations were obtained but are believed to be due to the aging of the photocathode. In fact, we noticed that in the last weeks of work (after approximately 300 hours of photocathode irradiation) the photocurrent values were around 10 times lower than their value at the beginning of the experiment for the same conditions. These lower current readings are more relevant in the case of low  $E/p$  above the photocathode, hence this was more significant in the measurements of REE variation with  $E/p$ . We tried to deal with this problem by repeating the measurement for several times and the average of these repetitions was obtained, being usually in accordance with what was expected.

## 6. Conclusion

The goals that were set for this work were the design and assembly of an experimental system that allows the measurement of the influence of the photon incidence angle in the extraction efficiency of reflective photocathodes at high pressure. This study was done for CsI photocathodes in Xenon gas for photon incidence angles from  $0^\circ$  to  $55^\circ$ .

The experimental system was designed with a very simple idea as the starting point but it allows other studies related to the incidence angle of photons in reflective photocathodes due to its versatility. These suggestions are developed in the next chapter.

The results obtained were satisfactory, and were obtained with great precision.

In this work, we studied a characteristic of CsI photocathodes that is not well described in the literature and obtained results that are in agreement with the suggestions of two of the three studies that we could find concerning the response of the quantum efficiency with the photon incidence angle.

An increase of the extraction efficiency with the photon incidence angle was obtained. An increase of  $\sim 35\%$  was obtained for a  $50^\circ$  incidence angle relative to the extraction efficiency value for  $0^\circ$ . This is in accordance with the work of Lopes and Conde [16] and Tremsin and Siegmund [18]. In their work they suggest that the increase of the quantum efficiency with the photon incidence angle is due to characteristics of the photocathode itself, such as the photoelectron production depth, and this is in accordance with what we obtained since we found that the REE dependence with the incidence angle was independent of the pressure of the Xenon gas and of the reduced electric field applied,  $E/p$ . Despite being compatible with these results for the case of gaseous Xe studied along this project time, it would be of interest to see if the behaviour observed in this study would remain the same in the presence of another gaseous atmosphere.

For the study of the REE dependence with the  $E/p$ , we obtained the expected results since our results show that extraction efficiency increases with the reduced electric field applied. This is in accordance to what is known from the literature, for example in [8] despite an effective comparison cannot be made since our values are only relative ones. This increasing behaviour was found to be independent of both pressure and photon incidence angle.



This work helped me to complete my formation as a Physics Engineer and it was an excellent way to finish my Master Degree. All the steps I went through during this work have provided me valuable experience for my future. The design of an entire experimental system, from scratch, and the development of a methodology in order to study something that I had never heard of was certainly a challenging but rewarding experience.

## 7. Future Work

Despite the accomplishment of the main purposes of this project, there are still several issues in the experimental system that could be improved in order to get more accurate results.

As already mentioned, one of the goals of this work was to build an experimental system capable of performing the study that was described. The system we developed has some perks that allow it, with just a few modifications, to be capable of answering most of these questions.

Hence, from my experience with this work, I leave here some ideas and suggestions for some future work that might follow my own.

One of the main drawbacks of the system is the difficulty it has in obtaining absolute measurements and this is due mainly to the difficulty in having knowledge of the intensity of the photons that impinge on the photocathode. Due to the residual pressure of the upper chamber, this intensity varies. This could be solved by connecting a vacuum gauge to this chamber to keeping track of the residual pressure in the chamber.

Another hypothesis would be to use a photodiode to measure the intensity of the light that hits the photocathode.

Following the work already done, we believe that would be wise to study the dependence of the extraction efficiency with the incidence angle for other different parameters of the reflective photocathodes such as, for example, its thickness and the substrate on which the photocathode is deposited.

Also it is important to perform this study in other gaseous atmospheres and also in vacuum since our measurements in vacuum were not possible.

Also, it would be of interest to complete this study with a spectral analysis of the light to see if the response of the REE with the incidence angle would change with the wavelength of the incidence light. In order to do this, the photon source in the experimental system should be changed or some filters could be added to the existing one.

One of the topics of interest concerning photocathodes is the aging effect, so could be interesting to study the influence of the known factors related to aging (such as

temperature, humidity and exposure to air) in the response to the incidence angle variation.

At last, I think it could be of relevance to study how different photocathode materials respond to the variation of the incidence angle. Although CsI is the most used one, there are other photocathodes with various applications for which it would be important to perform a study like the one made in this work for CsI.

## 8. References

- [1] Aprile, E., Bolotnikov, A. E., Bolozdynya, A. I., & Doke, T. (2004). *Noble Gas Detectors*.
- [2] Knoll, G. F. (2010). *Radiation Detection and Measurement* (4th ed.).
- [3] Lyashenko, A. (2009). *Development of gas-avalanche photomultipliers sensitive in the visible spectral range. Thesis*. WEIZMANN INSTITUTE OF SCIENCE.
- [4] Einstein, A. (1905). Über einen die Erzeugung und Verwandlung des Lichtes betreffenden heuristischen Gesichtspunkt. *Ann. Phys.*, 322(6), 132–148.
- [5] Spicer, W. E. (1958). Photoemissive, Photoconductive, and Optical Absorption Studies of Alkali-Antimony Compounds. *Phys. Rev.*, 112(1), 114–122.
- [6] Tamm, I. E. (1932). Photoemissive, Photoconductive, and Optical Absorption Studies of Alkali-Antimony Compounds. *Phys. Rev.*, 112(1), 114–122.
- [7] Escada, J. M. D. (2012). *Detetores Gasosos de Radiação: Efeitos da retrodifusão na emissão de fotoelétrons por fotocátodos de CsI em meio gasoso e eletroluminescência em Xe dopado com CH<sub>4</sub> e CF<sub>4</sub>*. UNIVERSITY OF COIMBRA.
- [8] Covita, D. S., et al. (2011). Photoelectron extraction efficiency from cesium iodide photocathodes in a pressurized atmosphere of argon and xenon up to 10 bar. *Physics Letters, Section B: Nuclear, Elementary Particle and High-Energy Physics*, 701(2), 151–154.
- [9] Escada, J., et al. (2010). A Monte Carlo study of photoelectron extraction efficiency from CsI photocathodes into Xe–CH<sub>4</sub> and Ne–CH<sub>4</sub> mixtures. *Journal of Physics D: Applied Physics*, 43(6), 065502.
- [10] Breskin, A. (1996). CsI UV photocathodes: History and mystery. *Nuclear Instruments and Methods in Physics Research, Section A: Accelerators, Spectrometers, Detectors and Associated Equipment*, 371(1-2), 116–136.

- [11] Coelho, L. C. C., et al. (2007). Measurement of the photoelectron-collection efficiency in noble gases and methane. *Nuclear Instruments and Methods in Physics Research, Section A: Accelerators, Spectrometers, Detectors and Associated Equipment*, 581(1-2 SPEC. ISS.), 190–193.
- [12] Triloki, et al. (2014). Photoemission and optical constant measurements of Cesium Iodide thin film photocathode. *Nuclear Inst. and Methods in Physics Research, A*, 787, 161–165.
- [13] Va'vra, J., et al. (1997). Study of CsI photocathodes: Volume resistivity and ageing. *Nuclear Instruments and Methods in Physics Research, Section A: Accelerators, Spectrometers, Detectors and Associated Equipment*, 387(1-2), 154–162.
- [14] Malamud, G., et al. (1993). Quantum efficiency and radiation resistance of bulk and porous CsI photocathodes in vacuum and methane. *Nuclear Inst. and Methods in Physics Research, A*, 335(1-2), 136–145.
- [15] Xie, Y., et al. (2012). Influence of air exposure on CsI photocathodes. *Nuclear Instruments and Methods in Physics Research, Section A: Accelerators, Spectrometers, Detectors and Associated Equipment*, 689, 79–86.
- [16] Lopes, J. A. M. and C. C. A. N. (1993). VUV efficiency of chevron type CsI vacuum photocathodes. *Journal Optics (Paris)*, 24(1), 15–18.
- [17] Miné, Ph., et al. (1995). Incident angle effect on the quantum efficiency of CsI photocathodes, 360, 430–431.
- [18] Tremsin, A. S., Siegmund, O. H. W. (1999). The dependence of quantum efficiency of alkali halide photocathodes on the radiation incidence angle. *Proceedings SPIE*, vol. 3765
- [19] FRASER, G. (1983). The characterisation of soft X-ray photocathodes in the wavelength band 1-300 Å. *Nuclear Instruments and Methods*, 206, 251–263.
- [20] HAMAMATSU. Deuterium Lamps - L2D2 Lamps.
- [21] Willistein, D. (2006). An Introduction to Optical Window Design. *University of Arizona, Introductory Opto-Mechanical Engineering*

- [22] Espe, W., Knoll, M., Wilder, M. P. (1951). Getter materials for electron tubes. *Vacuum*
- [23] SAES, “St 707 Non Evaporable Getters Activatable at Low Temperatures.”
- [24] Valentini, A. (2002). Influence of the substrate reflectance on the quantum efficiency of thin CsI photocathodes. *Nuclear Instruments and Methods in Physics Research Section A: Accelerators, Spectrometers, Detectors and Associated Equipment*, 482(1-2), 238–243
- [25] Bevington, P. R., & Robinson, D. K. (2003). *Data Reduction and Error Analysis for the Physical Sciences*. (McGraw-Hill, Ed.) (3rd ed.).
- [26] Forrestal, J. (1982). A compilation of Outgassing Data on Vacuum Materials.
- [27] Mamun, M. A. a., Elmustafa, A. a., Stutzman, M. L., Adderley, P. a., & Poelker, M. (2014). Effect of heat treatments and coatings on the outgassing rate of stainless steel chambers. *Journal of Vacuum Science & Technology A: Vacuum, Surfaces, and Films*, 32(2), 021604.
- [28] Leybold Vacuum. (2005). Symbols used in Vacuum Technology - Leybold Full line Vacuum Catalog.